Suppressor and calibration standard limitations in cation chromatography of ammonium and 10 alkylamines in atmospheric samples

Leyla Salehpoor and Trevor C. VandenBoer*

Department of Chemistry, York University, Toronto, ON, Canada.

Abstract

Ammonia (NH_3) and alkylamines are ubiquitous in the atmosphere and have been suggested to play important global roles through new particle formation and aerosol growth. In this work, we optimized an ion-chromatographic (IC) method to separate and quantify the ten most abundant atmospheric alkylamines with high selectivity and separation efficiency, using 4 μm packed columns and resin-based suppressors, alongside stabilizing amine standards. Modern resin suppressors operating on a gradient elution program affected the linear response of this IC technique. Calibration statistical analyses found a loss of analytes in these cation-exchange devices. Suppressor operational longevity was optimized by using a stepped current and an external water supply, which improved precision, accuracy, and LODs compared to other suppression modes. When this new method was applied to real samples, amines were found ubiquitously in size-resolved marine aerosol samples; monopropylamine, isomonopropylamine, and monobutylamine were detected and quantified in these samples, which have not been reported before. The molar ratio of the sum of aminium to ammonium ranged from 0.02 to 0.2, showcasing the application of the developed method towards studying the diversity and importance of alkylamines in coastal marine particle composition. The new analytical method also found NH_3 present in a suite of new homes with a mean mixing ratio of 25 ± 15 ppbv; a common level reached between homes across the study during the first year of occupation which can then be transported outdoors.

1. Introduction

Ammonia and alkylamines are reactive species ubiquitous in the atmosphere, emitted to the gas-phase in both outdoor and indoor air.[1] Outdoor sources originate from a variety of processes, both biogenic (ocean organisms,[2] biomass burning,[3] protein degradation,[4] and vegetation[5]) and anthropogenic (animal husbandry,[6] tobacco smoke,[7] industries,[8] combustion,[9] automobiles,[10] and treatment of sewage and waste[11]). The oceans emit these nitrogen-containing gases to the atmosphere due to biological degradation of organic matter, such as grazing of phytoplankton and remineralization of microorganisms, allowing them to contribute to the formation and growth of marine aerosols.[12] Global amine emissions are estimated at 285 ± 87 Gg N a^{-1} with 72% of terrestrial origin (205 Gg N a^{-1}) and 28% derived from oceanic sources (80 Gg N a^{-1}).[13] Methyl and ethyl amines (mono-, di-, and tri-) are the most abundant alkylamines in the atmosphere, with

higher concentrations in rural areas than in urban environments.[14] For example, global emissions of methylamines have been estimated at 150 ± 60 Gg N a^{-1} from animal husbandry operations.[5] Removal of amines from the atmosphere can proceed through gas phase chemical reactions, gas-to-particle partitioning, and wet deposition.[15] Amines are oxidized by reacting with the hydroxyl radical (OH), chlorine radical (Cl), nitrate radical (NO_3), and ozone (O_3) with short atmospheric lifetimes on the order of hours, mainly via loss to OH.[16] Amines can condense into the particle-phase and undergo neutralization reactions with acids such as HNO_3 and H_2SO_4, a process which has been suggested to play an essential role in new particle formation and aerosol growth.[17] Even though alkylamine concentrations are 1 – 3 orders of magnitude lower than NH_3 in the atmosphere, they compete with NH_3 to participate in these acid-base reactions.[15] This is in part due to alkylamines having higher basicity (pKa = 9.25–10.98) than NH_3 (pKa = 9.25), resulting in the formation of more stable salts, and by extension more rapid atmospheric particle formation. Amines can also undergo reactions with other organics in particles, like carbonyls, to form light-absorbing species such as imines, enamines, and even polymerized materials.[18] Formation of these high molecular weight nitrogen-containing products depends on the structure of the precursor amines (i.e. primary or secondary) and the presence of carbonyl compounds that can facilitate such particle formation or aerosol growth. De Haan *et al.*[19] measured the condensed-phase reactions between monomethylamine (MMA) and glyoxal to form oligomers, imidazole, and light-absorbing compounds that identified a new contribution for MMA to be involved in particle formation. In both cases, amines participating in the formation of new particles can go on to directly impact climate through their radiative forcing and indirectly by changing cloud droplet properties.[20,21] Changes in aerosol sizes and morphologies impact scattering and absorption of light, resulting in changes to aerosol photochemistry and the energy balance of Earth. Displacement reactions of ammonium by alkylamines, in contrast, improves sulfate aerosol water uptake and thereby their propensity to form cloud condensation nuclei (CCN). The formed CCN impact cloud formation and lifetime, and ultimately climate forcing through their radiative properties. Finally, gaseous amines can also be removed from the atmosphere through wet deposition in the form of rainwater and fogwater due to their high water solubility and acid-neutralizing capacity,[22,23] alongside scavenged aerosols.[24,25]

The study of ammonia and amines as atmospheric pollutants is also critical in indoor environments since people in North America spend more than 90% of their time inside yet the

sources and processes governing indoor air quality are poorly understood.[26] Ammonia and alkylamines have a number of indoor sources: tobacco smoke,[7] humans,[27] pet excrement,[28] cooking meat,[29] cleaners,[30] a host of consumer products,[30] and concrete curing agents.[31] The fate of indoor pollutants depends on environmental parameters such as humidity, temperature, the concentration of emitted compounds, air mixing, and air exchange by the ventilation system.[32] Ammonia and amines as gases or as components of inhalable particles have been associated with detrimental effects on respiratory health such as occupational asthma.[33] In indoor environments where nitrous acid is also abundant, amines may react to form toxic and carcinogenic nitrosamines.[34] Therefore, high quality analytical methods can play an important role in quantifying ammonia and amines indoors to help occupants recognize sources and reduce exposure to hazardous reaction products.

Analytical techniques to quantify NH_3 and alkylamines are essential in both aerosol and gas phases. Consequently, quantitative measurement of NH_3 and amines is required to understand their role in both phases in outdoor and indoor atmospheric environments. Amine-containing particles have been detected by multiple on-line mass spectrometric methods such as aerosol time-of-flight, atmospheric pressure interface time-of-flight, and thermal desorption chemical ionization.[35–38] The drawback of mass spectrometric measurements is that they provide qualitative results due to an inability to different structural isomers by their mass to charge ratio. These techniques can also be subject to substantial ionisation efficiency matrix effects. For example, Murphy *et al.*[39] observed increased ionisation efficiency of ammonia and amines in a C-TOF-AMS when methylamine was added to a chamber containing ammonium sulfate seed. Quantitative analysis of atmospheric alkylamines in gas and particle phases is challenging because of their low ambient concentrations (parts per trillion by volume (pptv)) in various environmental matrices.[13] Quantitative measurements of alkylamines have been obtained most often by chromatography methods such as gas chromatography (GC), high-performance liquid chromatography (HPLC), capillary electrophoresis (CE), and ion chromatography (IC). Most of these approaches (GC, HPLC, and CE) require extraction and derivatization to improve sensitivity, separation selectivity, and limits of detection, which is time-consuming and requires special handling when working with volatile compounds.[40–42] IC is regarded as one of the most common quantitative methods to analyze low molecular weight alkylamines, including tertiary amines, with the advantage of direct analysis of aqueous extracts, reducing sample preparation and contamination, analysis time, and

systematic errors.[43] However, previously developed IC methods could only analyze a few atmospheric alkylamines or struggled with coelution of pairs of cations (e.g. diethylamine ($DEAH^+$) and trimethylamine ($TMAH^+$)). Because of the low resolution and separation efficiency of prior IC methods,[39,44–47] Place *et al.*[48] developed the first successful IC method to separate the $DEAH^+$ and $TMAH^+$ pair, amongst others, by modifying the analytical column temperature for the separation. As a result, they could separate and quantify ammonium and the nine most abundant atmospheric alkylamines. Here we build on this prior work to develop an ion chromatographic method with conductivity detection (CD) to separate and quantify the ten most abundant atmospheric alkylamines (including MEtA) and six inorganic cations using the next generation of 4 μm stationary phase packing and dynamic suppression with resin-based ion exchange devices. Herein, we demonstrate an increase of separation efficiency and better peak resolution with gradient and temperature programming, an assessment of how to prepare stable calibration standards of alkylamines, an exploration of statistical approaches to recommend an appropriate calibration method that retains high accuracies for these analytes, an optimization of the suppression mode to obtain calibrations with the highest accuracy and precision outcomes alongside the lowest LODs, and application of the developed method to real atmospheric samples of aerosol and the gas phase to validate the IC method.

2. Experimental

2.1 Materials and Chemicals

A premixed cation standard concentrate (Dionex six-cation II, P/N: 046070, Thermo Scientific, Sunnyvale, CA, USA) of Li^+, Na^+, NH_4^+, K^+, Mg^{2+}, and Ca^{2+} was used to prepare inorganic cation stock solutions. Primary standard solutions of the following alkylamines: monomethylamine (MMA, 40% w/w), dimethylamine (DMA, 40% w/w), trimethylamine (TMA, 45% w/w), monoethylamine (MEA, 70% w/w), diethylamine (DEA, ≥ 99.5% w/w), triethylamine (TEA, ≥ 99.5% w/w), monopropylamine (MPA, ≥ 99% w/w), isomonopropylamine (iMPA, ≥ 99.5% w/w), monobutylamine (MBA, 99.5% w/w), monoethanolamine (MEtA, ≥ 98% w/w), and methane sulfonic acid reagent (0.1 M) were purchased from Sigma-Aldrich (Oakville, ON, Canada). Two analytical grade primary standard solutions of TMA and TEA chloride salts with concentrations of 1000 mg L^{-1} were purchased from the RICCA chemical company (CAT# RV010950-100N and RV010949-100N, Arlington, TX, USA).

2.2 Method Development for Separation of Alkylamines and Inorganic Cations

The chromatography method developed was based on a prior cation separation method using 5.5 μm particle sizes, electrolytic eluent generation, and an electrolytically regenerated suppressor.[48] Re-optimization of this IC method was required to separate and quantify the ten (including MEtA) most abundant atmospheric alkylamines and six inorganic cations. Therefore, several new innovations could be attempted to improve separation efficiency further and reduce method operating costs: 4 μm particle sizes in the analytical and guard columns, separated temperature controlled compartments for the columns and suppressor, the capacity to use a quarternary mixing valve to control eluent composition, and dynamically regenerated resin-based anion exchange suppressors. Samples were analyzed using a Thermo Scientific ICS-6000 IC-CD. A CS19-4 μm cation-exchange column was used to separate the suite of ten alkylamines and six inorganic cations (including ammonium, NH_4^+) by systematically exploring isocratic methane sulfonic acid (MSA) concentrations (1 to 10 mM), mobile phase flow rates (1.25 to 1.75 mL min^{-1}), and column temperatures (35 to 55 ºC). Maximum peak resolution was then further optimized by using a constant mobile phase flow rate of 1.25 mL min^{-1} and a 55 ºC column temperature. An eluent gradient was then constructed that resulted in optimized combination of peak resolution and run time as follows: initially hold at 1 mM over the first 20 mins, followed by a step increase to 4 mM before ramping exponentially to 8 mM over 5 mins, and holding for an additional 5 mins. Finally, the eluent was stepped back to 1 mM for equilibration over 5 mins before the next sample injection, yielding a total run time of 35 mins. Each sample injection consisted of 1 mL aqueous sample loaded onto a concentrator column (i.e. an inline cation exchange solid phase extraction column; TCC-ULP1; 5 x 23 mm, P/N: 01726065) and was performed with an autosampler (AS-DV). Analytes were injected by eluting them from the concentrator column with mobile phase and these were then separated on the guard (CG19-4 μm, 4 x 50 mm, P/N: 078840) and analytical columns (CS19-4 μm, 4 x 250 mm, P/N: 078837). The analytes were quantified using a conductivity detector (DS6 heated conducting cell at 35 ºC) after they passed through a resin-based anion exchange suppressor (CDRS 600, 4mm, P/N: 088668) temperature controlled at 15 ºC and operated in: i) dynamic mode, with a constant voltage of 4.4 V, or ii) legacy mode, with a stepped gradient current between 4 to 30 mA. Chromeleon™ v7.2.10 software was used to obtain the peak areas from each chromatogram. The data handling and calculation of concentrations were performed using a combination of Excel (O365, Microsoft Corp.) and Igor Pro (v8, Wavemetrics).

Some real atmospheric samples were analyzed using an isocratic method with an MSA concentration of 8 mM and a flow rate of 1 mL min^{-1} at a column temperature of 30 ºC where simple or known sample compositions were investigated. The same instrument components were employed for this isocratic method with the exception of larger packing sizes for the guard and analytical columns: CG19-5.5 µm (4 x 50 mm, P/N:076027) and CS19-5.5 µm (4 x 250 mm, P/N: 076026).

2.3 CDRS 600 Suppression Optimization

A dynamically regenerated suppressor was used for removal of eluent competing ions prior to the detection of inorganic cations and alkylamines (Fig. 1). Analytes are detected in their charged form in a water background. This technique dramatically improves instrument detection limits and is critical to optimize for trace analysis. Modern electrolytic suppressors can operate in two suppression modes to control the electrolytic current that replaces and neutralizes the eluent competing ions: i) dynamic, which applies a constant voltage to generate a responsive current based on eluent competing ion concentration and ii) legacy, which utilizes a current that is held constant. In a gradient method, dynamic suppression is considered more ideal than legacy because it adjusts current based on the competing ion concentration, thereby avoiding excess current being applied at lower starting eluent concentrations in gradients. There is no difference between the application of dynamic and legacy modes in isocratic methods, since both will maintain a constant current. The suppression of analytes eluting from the column with competing ions was initially performed with dynamic mode and water recycling (i.e. eluent exiting the detector was used for electrolysis of water in the suppressor) at a constant voltage of 4.4 V. Unfortunately, sensitivity of the method decreased over time, with concomitant loss of Mg^{2+} and Ca^{2+} ions occurring under routine suppressor operation. Alternatives to the suppressor methodology were explored for improved instrument performance.

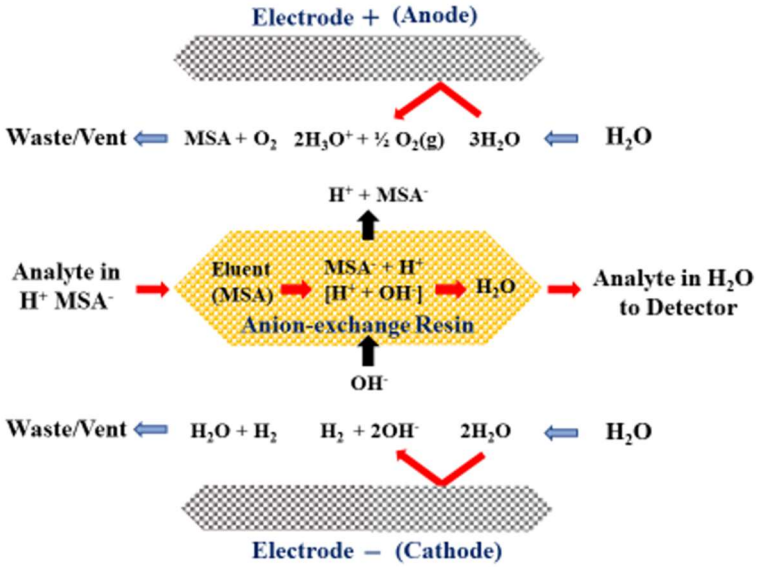

Fig. 1 Schematic of a cation dynamically regenerated suppressor (Thermo Scientific, CDRS 600). Deionized water is reduced to hydroxide ions electrolytically in the regenerant channel on the cathode surface by the constant applied voltage. Hydroxide ions move toward the anion exchange resin and neutralize H^+ competing ion in the eluent to form H_2O. Eluent anions (MSA^-) pass through the anion exchange resin by electromigration toward the anode where water is oxidized to produce hydronium ions that pair with the MSA^- to maintain electroneutrality. The analytes remain in the eluent stream because they are repelled at the positively charged anion-exchange resin, moving to the detector in pure water as a result, and measured as their conductive ions. Figure adapted from scheme for AutoSuppression found in Dionex CDRS 600 user's manual.[49]

To address this issue, the suppressor operation was changed from dynamic to legacy mode, programmed with different suppressor currents within legacy mode to effectively suppress the changes in eluent concentration in the IC gradient method, in addition to using water recycling or an external supply. In the cases where currents were modified, those used were calculated using formula (E1) recommended by the manufacturer, using the known eluent strength and typically applied as a constant to isocratic separations.

$$I = \mu \times C \times 2.94 \qquad \text{(E1)}$$

Where, suppressor current (I, mA) depends on mobile phase flow rate (μ, mL min^{-1}), eluent concentration (C, mN), and specific factor of 2.94 (mA min mL^{-1} mN^{-1}) that is based on sample counterion and mode of operation. As a result, step-wise changes in current over time were used as eluent ion increased in the gradient of a given IC separation method. For example, in our gradient approach with a flow of 1.25 mL min^{-1}, this corresponds to: 4 mA for 1 mM MSA, 15

mA for 4 mM, and 30 mA for 8 mM, as used below. A Chromeleon data file of the above-developed method is provided in the Supporting Information (Fig. S1).

Finally, the water supply of the suppressor in stepped-legacy mode was changed between being recycled or delivered from an external water supply. The aim was to obtain higher suppression capacity by more effectively removing all competing and analyte cations from the electrolytic compartments within the device (Fig. 1). Water provided from an external source was explored to reduce (or eliminate) the accumulation of low solubility salts in the suppressor that could damage the exchange resin (e.g. $Mg(OH)_2$ from Mg^{2+} in standards and samples) and other related processes (Section 3.5).

2.4 Quality Assurance and Quality Control (QA/QC)

2.4.1 Standards Preparation

Amine primary standard solutions were stored in 16 mL amber glass bottles because we observed their loss by volatilization was mitigated in these containers compared to high-density polyethylene (HDPE) bottles. There was also observable alteration of the HDPE containers (e.g. discolouration of material) as the analytes appeared to be permeating through the material, with reactive losses to impurities within it (e.g. reaction with carbonyls to form brown carbon products, such as in aerosol systems).[19] Aqueous working standards were stored in HDPE bottles cleaned with HPLC grade methanol and ultra-pure milli-Q water (DIW; resistivity of 18.2 MΩ·cm) by rinsing six times sequentially with each solvent. Standards were prepared in 50.0 ± 0.1 mL Nalgene™ class B polypropylene volumetric flasks with closure. To clean volumetric flasks, they were rinsed sequentially with methanol and DIW six times each before making standards.

2.4.2 Inorganic Cation Calibration Standards

Five calibration standards were prepared for inorganic cations by parallel dilution in DIW with the following ranges: Li^+ (5 to 99 ng), Na^+ (20 to 394 ng), NH_4^+ (25 to 498 ng), K^+ (50 to 990 ng), Mg^{2+} (25 to 502 ng), and Ca^{2+} (49 to 988 ng). The ranges describe the mass injected due to our use of a concentrator column. Two check standards were prepared within the calibration range positioned between the two highest (Li^+:74 ng, Na^+:296 ng, NH_4^+:374 ng, K^+: 743 ng, Mg^{2+}:377 ng , and Ca^{2+}: 741 ng) and two lowest (Li^+:7 ng, Na^+:30 ng, NH_4^+:37 ng, K^+: 74 ng, Mg^{2+}:38 ng, and Ca^{2+}: 74 ng) standards to evaluate method quality across the instrument working range.

Specifically, they were used here to determine accuracy through their percentage relative error (%RE) compared to the known concentration (n = 5).

2.4.3 Amine Standard Stability

We have previously noted that a limit on the accuracy in quantifying amines by IC is derived from the stability of standard solutions and potential losses of analytes from these standards.[44,48] The issue remains open and potential resolutions to improve quantitative analysis were explored. Three aqueous solutions of a mixture of alkylamines were prepared in both DIW and 1 mM MSA to assess whether improved stability in quantitation could be obtained by fixing the protonation of these basic analytes in an acidic solution matched to the matrix of the mobile phase under the starting conditions of the separation. The stability of alkylamine mixtures were tested by aging 10 mg L^{-1} stock solutions over short-term (up to 19 days) and long-term (>19 days) periods. The first mixture contained MEtA, DMA, DEA, and TEA, the second contained MMA, iMPA, and TMA, and the third contained MEA, MPA, and MBA. Amine analyte mixtures analyte were designed based on their determined elution order from single analyte standards, such that retention times for amines in a mixture were separated a few minutes from each other. In addition, solutions denoted TMA.HCl and TEA.HCl were prepared from chloride salts and compared to those made from their primary standard solutions (denoted TMA and TEA above) in terms of stability as these analytes have demonstrated the lowest accuracy and precision in our prior work. Five standard solutions of the amine mixtures were made by combination of both parallel and serial dilution, to practically reduce error in both DIW and MSA matrices, with calibration ranges between 5 to 500 ng injected on-column. The stability of the amines standard stock solutions was tested first by measuring instrumental sensitivity through calibration standards and then by comparing the experimental decay rates to the relative effective volatilities of the analytes ($K_{eff} = K_a/K_H$) in both matrices over 90 days. This comparison explores the idea that the main loss in our prepared amine standards is through volatilization. One check standard was prepared from stock standards that was made freshly with mass of 50 ng from primary standard solutions with a concentration of 50 ng mL^{-1} to assess the accuracy of the resulting amine calibration curves (n = 5).

2.4.4 Precision and Limits of Detection

The method precision of inorganic cations and amine calibration standards was calculated using the standard deviation (σ) in the slope (sensitivity) of the linear calibration curves across multiple analyses spanning several months. Method precision was alternatively calculated through the replicate analysis of check standards in the cases where there were not enough replicates of full calibrations using standards due to clear and rapid damage of the suppressor (i.e. total loss of function after tens of injections, indicated below with an asterisk*; called *critical failure* henceforth). Precision was determined for each of the configurations in suppressor operation and regenerant water provision: dynamic recycle (n = 3 inorganic cations, n = 5* amines), stepped-legacy recycle (n = 5* inorganic cations, n = 5* amines), and stepped-legacy external (n = 5 inorganic cations, n = 3 amines).

Limits of detection (LOD) for inorganic cations and alkylamines were determined using calibration standards and three reagent blank chromatograms under all three suppressor configurations. The LODs were calculated in nanomoles (nmol) using the ratio of three times the standard deviation of the blank signal height from the detector (μS) within the analyte retention time window where no peaks were observed. The resulting value was divided by the slope of the calibration curve when plotting standard peak height versus nmol of analyte injected ($\mu S\ nmol^{-1}$). The LOD determinations were performed using a brand-new suppressor with a detector data collection rate of 10 Hz, and resulted in up to 358 data points within the various analyte retention windows (e.g. n = 263 for Li^+ and n = 188 for K^+, where the retention windows were determined from the average ion retention time across the calibrated linear range ±3σ).

2.4.5 Assessment of the Calibration Approach for Quantitative Analysis

Method validation indicates whether the performance of a newly developed method is reliable and consistent for data analysis.[50] Calibrations are one of the most important parameters where mistakes can be made in regression when including the zero-point (0,0) and forcing the line through the origin. Without the incorporation of reagent blank analyses, including (0,0) in a calibration curve can be a source of error since most analytical instruments generate a non-zero background signal. The only exception of using the zero-point is chromatographic techniques where a reagent blank has been run and no signal has been detected (i.e. <LOD).[51] Regression through the origin is usually used for simplicity of the calculation, as there is no y-intercept value. There has been controversy about this topic without clear conclusions.[52] One consensus is that a

calibration curve can only be forced through the origin when there are no significant differences between y-intercept and zero from a unrestricted linear least-squares regression. In this study, injection of DIW as a reagent blank and statistical approaches from the literature were performed to evaluate the best practice in use of inorganic cation and alkylamine calibration curves with the modern components of cation-exchange chromatography instrumentation. Details of statistical approaches considered for the regression analysis are presented in the SI (Section S2).

2.5 Analysis of Real Samples

Our developed IC methods were applied to quantify NH_3 and alkylamines in real samples of outdoor aerosols and the gas phase indoors to demonstrate its sensitivity and robustness.

2.5.1 Size-Resolved Coastal Aerosol Sample Analysis

Analysis of particulate-phase NH_4^+ and amines in marine aerosols with an improved IC-CD method is essential to further our understanding of the sources and sinks of reduced nitrogen in the marine atmosphere. Size-resolved aerosol samples were collected with a Micro Orifice Uniform Deposit Impactor (MOUDI, model 100-NR, MSP Corp., Shoreview, MN, USA) during the Coastal Fog cruise that travelled along the coast of Eastern Canada in September 2018.[53] The MOUDI was operated at a sampling flow rate of 30 L min^{-1} with 9 impaction stages set-up to capture particle fractions with aerodynamic diameters centred at 0.18, 0.32, 0.56, 1.0, 1.8, 3.2, 5.6, 10, and 18 μm. Nine rounds of 24-hour aerosol sampling were conducted across various parts of the Grand Banks region, including the open ocean (5 samples), the Gulf of the St. Lawrence (2 samples), and in urban harbours (2 samples). Samples were collected on pre-cleaned 47 mm aluminium foils, which were soaked in DIW for 10 – 60 min and then sonicated for 20 min, followed by sampling, and then extraction in to 15 mL of deionized water with 45 min of sonication and centrifugation at 6000 rpm for 20 min. The extracts were then analyzed using the best IC-CD gradient method available at that time (see Section 3.7). More detailed information about MOUDI samples, their broader chemical composition, and impacts on coastal and marine atmospheres can be found in Chisholm *et al.*[54]

2.5.2 New Home Air Quality Sample Analysis

The developed IC-CD methods were used to measure the indoor concentration of NH_3 and amines to explore their temporal variability and the effect of occupant activities and household components on their levels in the first-year of occupancy in new homes. The mixing ratios of gaseous NH_3 and amines were measured in 18 newly constructed homes in the Ottawa-Gatineau (Ontario, Canada) census metropolitan area between 2018 and 2022. Samples were collected before and immediately upon occupancy (24-hour duration) and at 3-month intervals thereafter (each 5 days in duration) for the first year, using Ogawa passive samplers (PS-154, Ogawa & Co. USA, Inc., Pompano Beach, Florida) with citric acid-coated reactive substrates.[55] A total of 7-8 sample substrates were collected indoors (n=4), outdoors (n=2) and as field blanks (n=1-2) at each home, for each timepoint. All the substrates were extracted by being placed in 15 mL deionized water and mixed intermittently by several inversions over an hour, followed by analysis using IC-CD. Half of the samples were analyzed with the gradient method and the remainder with the isocratic method, to preserve suppressor function (Section 3.8).

Results and Discussion

3.1 Advancing Separation of Alkyl Amines

An improvement in resolution and quantitation of alkylamines, expanding the analyte suite to include MEtA, was explored based on the cation gradient separation of Place *et al.*[48] applied to various modifications to the analytical column and suppressor. These modifications including using the newly available 4 µm packing instead of 5.5 µm in the CS19 analytical column, utilizing separated temperature controlled compartments for the column and suppressor instead of a single compartment, incorporating a quarternary mixing valve, and using a dynamically regenerated resin based suppressor instead of an electrolytically regenerated suppressor that was limited to legacy mode. The selectivity of the stationary phase was exploited for this compound class, starting from the optimal hydronium ion (H_3O^+) gradient and flow rate determined in our prior work. From this point, temperature modulation spanning 35 °C to 55 °C in 10 °C increments was optimized, as we have also previously determined that this parameter exerts a strong effect on selectivity.[48] The effect of the temperature on peak separation was then assessed by calculating the peak-to-peak resolution (E2) for each consecutive pair of cations.[56]

$$R_s = \frac{2(t_{R2}-t_{R1})}{W_2+W_1} \quad \text{(E2)}$$

Where t_R is retention time (min) and W is peak width at the base (min). The resolution averages of inorganic cations and ten alkylamines were 1.10 ± 0.97, 1.45 ± 0.82, at 35 °C, 45 °C, and 1.52 ± 0.81 (dynamic recycled water) and 2.30 ± 1.69 (legacy external water) at 55 °C, respectively (Table1).

Table 1: Peak-to-peak resolution of inorganic cations and ten alkylamines from the following analyte at different column temperatures increases the selectivity of the stationary phase.

	Resolution			
Cation	35 °C (DR)[c]	45 °C (DR)[c]	55 °C (DR)[c]	55 °C (LE)[d]
Li^+	3.71	2.98	2.68	4.24
Na^+	2.03	1.72	1.69	2.83
NH_4^+	1.33	1.32	1.27	1.01
$MEtAH^+$	0.51	1.36	0.86	1.42
$MMAH^+$	1.18	1.04[a]	0.88[a]	1.20[a]
$MEAH^+(K^+)$ [a]	0.98	0.64[a]	0.71[a]	0.77[a]
K^+ $(MEAH^+)$ [a]	0.98	0.46[a]	1.02[a]	1.12[a]
$DMAH^+$	0.02	1.56	1.35	1.94
$iMPAH^+$	0.38	1.77	1.66	1.05
$MPAH^+$	0.46	0.97	1.11[b]	1.26[b]
$DEAH^+$	0.15	0.24	0.95[b]	0.84[b]
$TMAH^+$	1.32	2.76	3.43[b]	4.01[b]
$MBAH^+$	1.27	2.07	2.17	6.08
$TEAH^+$	---	---	---	4.81
Mg^{2+}	---	---	---	1.90
Ca^{2+}	---	---	---	---
Average	1.10	1.45	1.52	2.30

[a] K^+ elutes before $MEAH^+$. R values calculated between $MMAH^+$ and K^+, K^+ and $MEAH^+$, and $MEAH^+$ and $DMAH^+$.
[b] $TMAH^+$ elutes before $DEAH^+$. R values calculated between $MPAH^+$ and $TMAH^+$, $TMAH^+$ and $DEAH^+$, and $DEAH^+$ and $MBAH^+$.
[c] Peaks evaluated at a mass of 326–991 ng (alkyl amines) and 74–743 ng (inorganic cations) with the suppressor operated in dynamic recycle mode (DR).
[d] Peaks for final optimized method (stepped-legacy external water = LE) evaluated at a mass of 500 ng (amines) and 74–743 ng (inorganic cations) for comparison to method performance of Place et al.[48]

Resolution between inorganic cations and amines was enhanced by increasing the temperature and changing suppressor modes from dynamic with recycled water to stepped-legacy with externally supplied water (Table 1). Coelution between K^+ and its neighbouring amines was a consistent issue at temperatures below 50 °C, which was overcome above this value. The greatest resolution improvement was observed between $DEAH^+$ and $TMAH^+$, which had poor separation

below 55 °C. The chromatograms of the suite of four inorganic cations and ten alkylamines expected in atmospheric samples shows their successful separation from a modest change in column temperature to 55 °C from 45 °C (Fig. S2). The chromatograms demonstrate improvement in peak shape and separation efficiency at 55 °C, consistent with prior findings that the biggest driver of selectivity in modern cation separation of alkylamines is temperature, as selectivity is insufficient at the weakest possible competing ion concentrations in the mobile phase. Additionally, the suppressor operational mode impacts the resolution at the optimized temperature of 55 °C; changing the suppressor from dynamic recycled water to stepped-legacy external water resulted in an average resolution improvement by a factor of 1.5 (Table 1).

Drawing from the fundamental components of the van Deemter equation (E3), the improved resolution in the cation separation by increasing temperature can be better understood.

$$H = A + \frac{B}{\mu} + (C_S + C_M)\,\mu \qquad \text{(E3)}$$

Where H is the theoretical plate height (inversely proportional to plate number), A is the eddy diffusion coefficient, B is the longitudinal diffusion coefficient, C is the mass transfer coefficient in the stationary (C_S) and mobile (C_M) phases, and μ is the flow rate. [57–59] By increasing the column temperature, the viscosity of the mobile phase was decreased, and mass transfer increased with diffusion through the stagnant mobile phase inside the porous particles.[60,61] Increasing temperature also enhances the ion desorption kinetics of the stationary phase.[62–64] The cumulative impact of these effects reduces the C_S term. An increase in analyte diffusion in the mobile phase also results in a decrease of C_M term. Together both decreasing C terms lead to increased efficiency. In this experiment, an increase in peak resolution resulted when the mobile phase had greater diffusivity, with best separation efficiency at a temperature bordering on the limit for the CS19 column (60 °C). Elevated temperature further reduces retention time by changing the retention enthalpy of the analyte and/or the degree of ionization of the solute and functional group of the stationary phase.[59,61] For example, here the retention times of the cation analytes decreased anywhere from 0.25 (Na^+) to 2.43 ($TMAH^+$) minutes when increasing the temperature from 45 °C to 55 °C with the suppressor operated in dynamic recycled water mode (Fig. S2). Also, increasing temperature affected peak widths by reducing them from 0.02 (Li^+) up to 0.41 ($MPAH^+$) minutes, suggesting substantial mass transfer band broadening effects (C-term) in these separations. Lastly, increased temperature resulted in an improvement of the peak shape, with a reduced extent of peak tailing

particularly for early eluting analytes, as quantified by the asymmetry factor, which is the sum of the left and right peak widths at 5% of the peak height in minutes, divided by the left peak width at 5% of peak height in minutes multiplied by 2. These decreased from 1.59 to 1.14 for $MMAH^+$ and up to 2.53 to 1.01 for Li^+, improving across the entire analyte suite. In a previous study, it was shown that a change in temperature (60 °C) elicits an effect similar to that of adding an organic modifier (6% acetonitrile) to improve the separation efficiency of amines.[65] However, there are organic solvent limitations for suppressors and electrolytic eluent generators used on modern IC systems, so temperature alterations provide the benefit of similar improvements in selectivity, while remaining compatible with these components. In summary, elevated temperature improved chromatographic peak shape with better symmetry and reduced peak width. Overall, the higher temperature of the final method strongly altered the selectivity of the CS19 column, perhaps best indicated by the reversal of the elution order for $DEAH^+$ and $TMAH^+$.

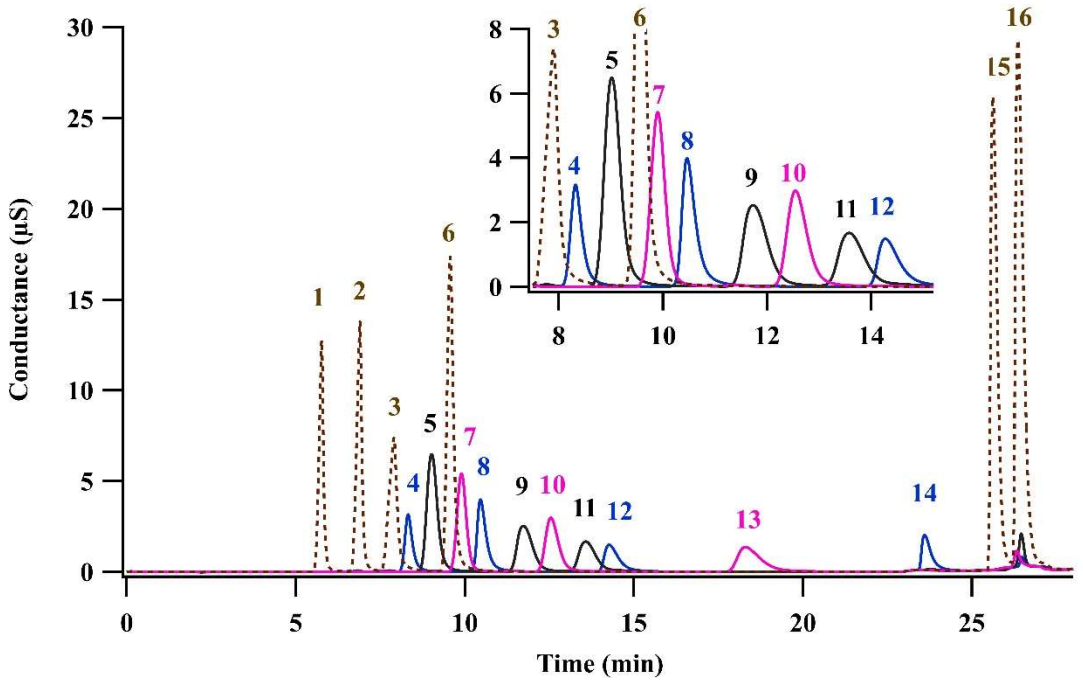

Fig. 2. Separation of inorganic cations and three amine mixtures with an MSA gradient from 1-8 mM and flow rate of 1.25 mL min^{-1} at 55 °C. Analytes were passed through a suppressor in stepped-legacy external water mode before detection (final optimized method). Inorganic cations and three amine mixtures are coloured separately: dashed trace (inorganic cations), blue solid trace ($MEtAH^+$, $DMAH^+$, $DEAH^+$, $TEAH^+$), black solid trace ($MMAH^+$, $iMPAH^+$, $TMAH^+$), and pink solid trace ($MEAH^+$, $MPAH^+$, $MBAH^+$). The identity, numeric order of elution, and mass of each cation separated are: Li^+ (1, 74 ng), Na^+ (2, 296 ng), NH_4^+ (3, 374 ng), $MEtAH^+$ (4, 500 ng), $MMAH^+$ (5, 500 ng), K^+ (6, 743 ng), $MEAH^+$ (7, 500 ng), $DMAH^+$ (8, 500 ng), $iMPAH^+$ (9, 500

ng), $MPAH^+$ (10, 500 ng), $TMAH^+$ (11, 500 ng), $DEAH^+$ (12, 500 ng), $MBAH^+$ (13, 500 ng), $TEAH^+$ (14, 500 ng), Mg^{2+} (15, 377 ng), and Ca^{2+} (16, 741 ng).

In this work, we tried to improve the IC method further in its application to separate the atmospherically relevant suite of six inorganic cations and ten alkylamines at 55 °C in stepped-legacy external water mode (Fig. 2). This separation was performed through the reduced particle size now available at 4 μm instead of 5.5 μm in analytical columns used previously.[48] Theoretical plate height is directly proportional to the diameter of stationary phase particles ($2d_p + d_p^2$); therefore, it was expected H should decrease by a factor of 1.7.[66] Improvement in theoretical plate number was observed for most of the analytes (9 out of 16): six inorganic cations, $MEtAH^+$, $DMAH^+$, and $TEAH^+$. For example, the H value of NH_4^+ was calculated from our method using E4 as 0.11 mm using the 4 μm packing, a decrease in H by a factor of 1.4 compared to the value of 0.15 mm using the 5.5 μm packing.

$$H = \frac{L}{N} = \frac{L\,W^2}{16\,t_R{}^2} \quad \text{(E4)}$$

Where L is the column length (mm). Separation efficiency did not change in three alkylamines: $MMAH^+$, $MEAH^+$, and $DEAH^+$, while the remaining four ($iMPAH^+$, $MPAH^+$, and $MBAH^+$) had decreased. This IC method also observed an improvement, for example, in the resolution of $MEtAH^+$ from NH_4^+ and $MMAH^+$ which had R_s values less than 0.65 increase to 1.01 and 1.42, respectively. Improvement in selectivity is yet required for some of analyte pairs, such as K^+ and $MEAH^+$, but was not possible to achieve within the stationary phase limits here. The expected improvement in separation efficiency from the reduced stationary phase particle size found are consistent with the expected theoretical improvement, a substantial impact for this analyte suite.

3.2 Stability of Amine Standards

The stability of amine standards was measured over time to explore the potential impact of volatility driven losses on the accuracy and precision of TMA specifically, which was an outstanding issue reported in our previous IC methods.[44,48] As a result, an investigation of fixing the ionized state of all the analytes in the samples was designed to ascertain whether this is the case, or if the observed losses are occurring elsewhere in the instrumentation. The stability of standards was tested by changing the pH with MSA or preparing standard solutions from the hydrochloride salts, such as TMA.HCl and TEA.HCl. Instrumental sensitivity to the inorganic

cations and amines were measured over 90 days in two groups: short-term (up to 19 days) and long-term (> 19 days) when stored in DIW or MSA and subject to the conditions present from three different suppressor modes (Fig. S3). Stock standard solutions (10 mg L^{-1}) were used to evaluate stability through sensitivity changes, which were quantified using calibration standards prepared from the stock solutions. Potassium sensitivity was observed to change over the course of the IC-CD analyses performed across these varied instrumental configurations and within one suppressor over time, despite it being known to be a conserved ion. As a result, it can account for system performance variability over time. This was exploited to obtain comparability between suppressor operation modes and stock solution matrices in our stability tests and the sensitivities of all analytes prepared in DIW or MSA were therefore normalized to K^+ sensitivity, in particular to account for the degradation of suppressor performance (Section 3.4.2). This is a reasonable approach toward mitigating changing instrument function as the relative difference between DIW and MSA matrix sensitivities for K^+ were 9 % which is within the typical analytical accuracy reported for IC instrumentation.[44,48] Furthermore, we selected this particular conserved inorganic cation from our suite because K^+ has the nearest retention time to most of the amines, such that suppressor performance was best accounted for on an injection-to-injection basis (Table 1, Fig. 2).

Under these constraints, it was possible to assess the stability of amine standards over time as well as the potential stabilizing effect of an acidified standard matrix using the same competing ion as found in the mobile phase (MSA, Fig. 3). Short-term stability is essential to assess if amines have the same stability as inorganic cation standards, where the latter can be stored in a stock solution for up to three weeks.

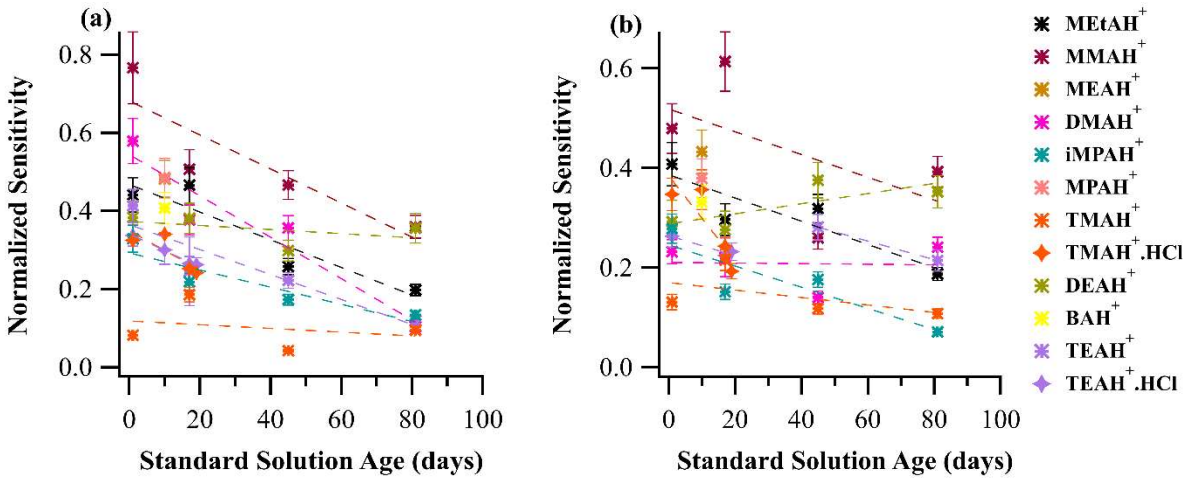

Fig. 3 Sensitivity of alkyl amines relative to K^+ measured using calibration standards with different ages of the used stock solution in (a) DIW and (b) MSA. Here, all measurements were made by using the same suppressor in dynamic mode with recycled water.

In DIW, the sensitivity of amines decreased over time, and the measured instrument response decreased for $MMAH^+$, $DMAH^+$, $iMPAH^+$, $TMAH^+$.HCl, $TEAH^+$, and $TEAH^+$.HCl indicating analyte degradation or losses – with an average percentage loss of 30 ± 10 % over the short-term experiment (up to 19 days). In contrast, the normalized sensitivities measured for $MEtAH^+$ (0.44 ± 0.04 and 0.46 ± 0.04) and $DEAH^+$ (0.38 ± 0.04 and 0.38 ± 0.03) demonstrated high stability, without a significant change during the short-term observation period. $TMAH^+$ did not show a similar instrument response as the other amines, and its high variance was therefore investigated to be due to its loss from the IC system (Section 3.3.2). In the MSA matrix, $MEtAH^+$, $iMPAH^+$, $TMAH^+$.HCl, and $TEAH^+$.HCl showed declining instrument response over time with an average loss of 29 ± 13 % in the short-term. Meanwhile, $MMAH^+$ and $TMAH^+$ did not show any consistent pattern and they fluctuated by up to 28% and 64% from the initial measurement respectively over the observation period. Finally, $DMAH^+$ and $DEAH^+$ were observed to have the highest stabilities over the same short-term period. In the short term, storing amine stock standard solutions in DIW resulted in greater retention of instrumental method sensitivity compared to storing them in MSA (MSA/DIW<1; Fig. 4). In contrast, instrumental method sensitivity of stock solutions in MSA relative to DIW were less impacted at longer timescales (MSA/DIW >1) despite the significant losses observed in both systems over time. In summary, the highest instrumental method sensitivity, accompanied by reproducibility, can only be obtained by preparing freshly made amine stock solutions from the primary standards, on the day of quantitative analysis for samples of unknown composition, using a simple matrix of DIW.

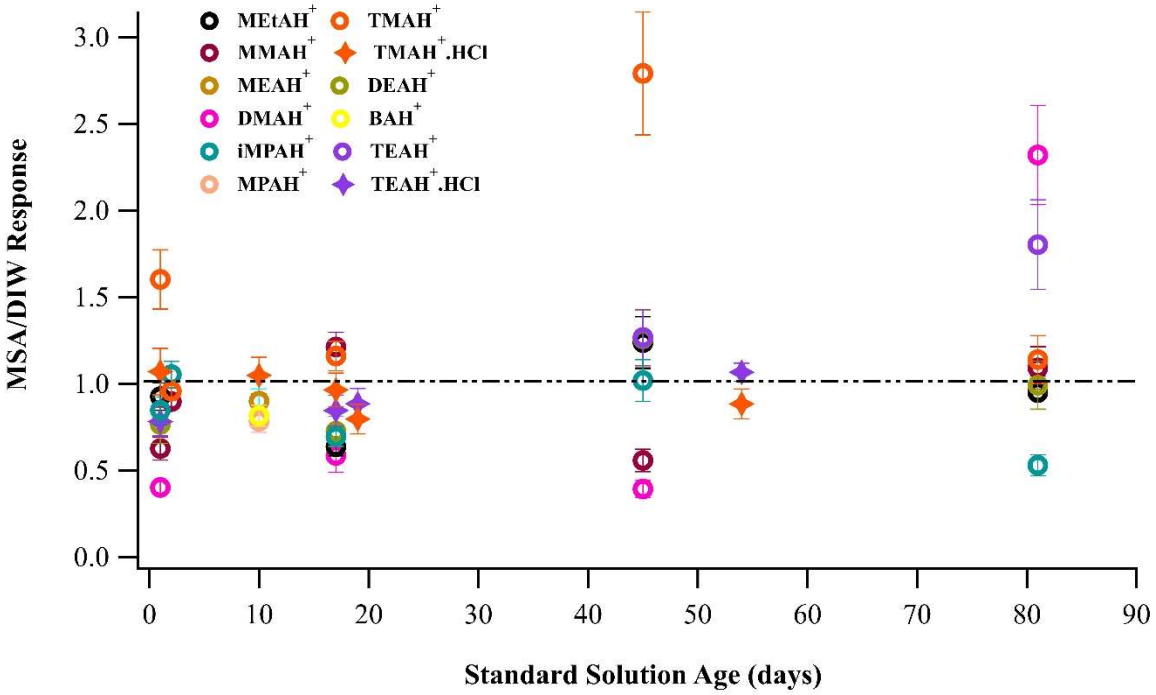

Fig. 4 Ratio of amine sensitivities in DIW-to-MSA at different stock solution ages, as quantified by one suppressor operated in dynamic mode with recycled .

Amine stock standard solutions of the hydrochloride salts indicated similar instrumental sensitivity in DIW and MSA (MSA/DIW ≈1) over short- and long-term storage. However, due to the quantities of these analytes lost over time freshly made stock solutions are still required to obtain the correct instrument response with reproducibility.

Decay rate of amines (day^{-1}) were measured by plotting natural logarithm of the normalized amine sensitivities relative to K^+ versus their age in days (e.g. $iMPAH^+$ in Fig. S4). The loss was first-order in nature and decay rates were determined from the slope. It was expected that the amine decay rates would be slower in MSA than in DIW if volatilization was the dominant loss mechanism, as the analytes would be mostly protonated (99.99 %) in a 1 mM MSA solution (pH = 3) compared to pure water (68% for MEtA to 99% for DEA) (Fig. 5).

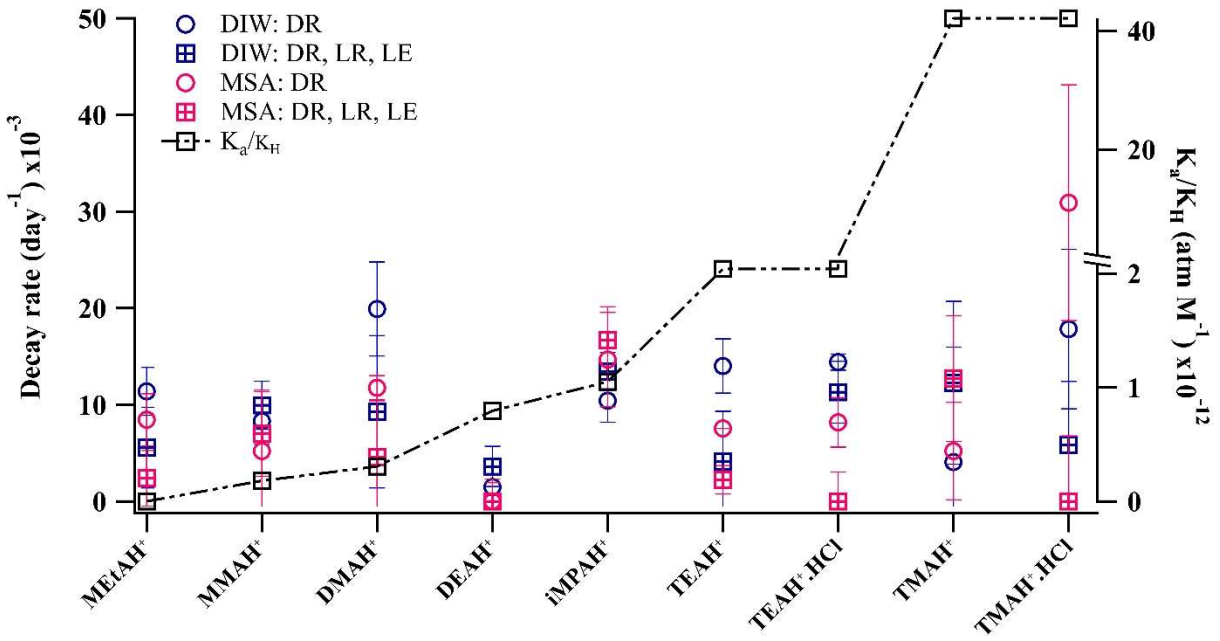

Fig. 5 The stability of amine standard stock solutions comparing experimental decay rates to a proxy for volatilization loss. Experimentally determined decay rates of the amine analyte suite in both DIW and MSA were measured using the same suppressor in dynamic (D) mode with recycled (R) water as well as other suppressor configurations such as stepped-legacy (L) recycle and external (E) water modes (left axis). The theoretical decay rates via volatilization for the same amines based on their K_a and K_H values were also calculated for comparison (right) axis. Note the axis break on the right changing the order of magnitude in the scale for TMA.

For comparison, we derived the theoretical relative loss potential of each amine by volatilization based on their combined acid ionization constant of the conjugate acid (K_a) and Henry's Law constant (K_H = M atm^{-1}) (SI, Table S3).[67–69] The degree of amine partitioning from the aqueous to the gas phase at equilibrium is thus based on R1 and R2.

$$NR_3H^+_{(aq)} + H_2O_{(l)} \rightleftharpoons NR_{3(aq)} + H_3O^+_{(aq)} \quad \text{(R1)}$$

$$NR_{3(aq)} \rightleftharpoons NR_{3(g)} \quad \text{(R2)}$$

As a result, it would be expected that the amine decay rates are dependent on the ratio of K_a to K_H if this is the driving process. The order of theoretical loss of amines due to volatilization increases from $MEtAH^+$ as the lowest to $TMAH^+$ as the highest (Fig. 5). Based on the hypothesis that this property is the main driver of analyte loss in standard solutions, it was expected that the stock standard of $MEtAH^+$ would be the most stable over time with an increase in loss and/or variability towards the more volatile analytes like $TMAH^+$; the most volatile of the analyte suite. The decay rates were compared across different supressor modes which showed similar variabilities in amine

decay rates. Diethylamine ($DEAH^+$) is the most stable analyte in the suite, with decay rates close to zero, without measurable losses under our instrumental conditions. In contrast, all other amines show high variability with respect to losses during storage of stock solutions with measurable decay rates. The loss of analytes was still observed in cases where the solution pH was lowered, as well as when starting with an ionized reagent through chloride salts, despite the expectation that they would maintain their charged form. Linear regression analysis of amines experimental decay rates versus K_a/K_H showed no correlation ($R^2<0.2$ in all cases) between these variables for and of the different suppressor modes. The slope of the regression lines in MSA was positive and higher than DIW; MSA was not more effective than DIW in preventing losses. This result suggests that other factors than volatilization of the neutral amines are affecting the decay rate, such as analyte loss from the suppressor (Section 3.3.1). Again, our results suggest that all amine stock standards need to be freshly made from the primary standard solutions prior to each analytical determination to ensure high quality quantitative results.

Place *et al.*[48] observed lowest accuracy in analytical determinations of $TMAH^+$ and $DMAH^+$ (at the lower end of the calibrated range), alongside the largest variations in the slopes of calibration curves of $TMAH^+$ and $TEAH^+$ over one to three months. In that prior work, the losses were hypothesized to be driven by volatilization from the standards. In the experiment conducted here, the highest variability is observed in these same three amine standards: $TMAH^+$, $DMAH^+$, and $TEAH^+$, but the effects do not scale with the known effective volatility of these molecules. High variability of the $DMAH^+$ decay rate could be associated with the loss of this amine from the suppressor, particularly when it was operated under dynamic recycle water mode (Section 3.3.1). Standard solutions of TMA.HCl and TEA.HCl from freshly made stock solution were used to verify the stability of the freshly made standard solutions of TMA and TEA. Stability of TMA and TEA were then explored by comparison to TMA.HCl and TEA.HCl as the stable form of standard solutions under different suppressor modes. The analytical sensitivity of $TMAH^+$ was lower by 67% (dynamic recycle), and 28% (stepped-legacy external) when compared to $TMAH^+$.HCl. The sensitivity differences between $TEAH^+$ and its chloride salt was 18% (dynamic recycle), 1% (stepped-legacy recycle), and 15% (stepped-legacy external). These results indicate that the lower instrumental method sensitivity of TMA compared to TMA.HCl may be due to a combination of factors: i) TMA has higher volatility and is susceptible to loss when preparing stock solutions and ii) the suppressor mode and supply water format lead to amine losses in the eluate from analytical

IC column. Therefore, to negate the first issue, and obtain high quality quantitative analysis of high volatility amines like TMA and TEA, we recommend preparation of aqueous stock standards from their hydrochloride salts prior to each instrument calibration.

3.3 Optimizing Calibration Approaches with Different Suppression Modes

Regression lines for calibration standards were fitted by applying the calibration method from previous IC studies: forcing the regression line through the origin after background correction for any signal in the reagent blank.[44,48] Here, we found the linearities of our calibration curves to be much different by assessment of the residuals and through use of check standards, which was eventually linked to the operation parameters of the suppressor. Statistical considerations were then made to evaluate the best practice in quantifying cations when using external calibration curves for the new generation of resin suppressors.

3.3.1 Inorganic Cation Standards

Since reagent blanks were injected along with the inorganic cation standards, the resulting calibration peak areas were corrected by background subtraction of any peak areas observed in the reagent blank. As a result, it is analytically acceptable that the zero-point could be used for curve generation in this calibration approach. Three different types of linear calibration curves were then utilized and their regressions were: i) forced through (0,0), ii) not forced through origin but included (0,0) in the regression, and iii) not forced through the origin and not inclusive of (0,0) (Fig. S5). A linear least-squares regression fit (R^2) of the calibration standards (n = 5) and the percent relative error (RE %; the difference between the known and calculated concentrations) of the check standards (n = 2) were used to assess accuracy between the three calibration strategies. In the first approach, the regression lines forced through zero resulted in R^2 values ranging from 0.943 to 0.953 and a RE % of -27 ~ +5. In the second approach, it was found that not forcing through zero but including (0,0), improved R^2 values between 0.997 to 0.998 and a RE % of -7 ~ +13. In the third method, not forcing through zero and excluding (0,0) increased R^2 from 0.998 to 0.999 and had RE % of -5 ~ +29. The most accurate calibration strategy was the second approach, where the zero-point was included but the regression line was not forced through the origin. This is consistent with the finding that the analytical accuracy of IC, when data is interpreted with a

suitable calibration approach, is generally within 20% of the known value of a suitable check standard.[44,48]

Even though the second approach gave us the most accurate calibration curves by not forcing through zero, one should statistically test to confirm whether the intercept values of these calibration curves are significantly different from zero. To determine the significance of the y-intercept, three different statistical approaches can be used: i) test statistic (t-statistic), ii) confidence interval of the y-intercept, and iii) standard error of the intercept.[50,51] The values of all three above-mentioned approaches are presented in Tables S1 and S2. The results of approaches i) and ii) used a t-statistic and the confidence interval of the y-intercept to accept the null hypothesis that the y-intercept value is insignificant. However, the approach of iii) rejects this null hypothesis and confirms the y-intercept to be significantly different from the standard error of the y-intercept. Negative intercepts were observed in linear regression lines of the inorganic cations which indicates that analytes were lost in the IC system, something that can only occur in the anion-exchange resin of the suppressor (Fig. 1). The loss of analytes was calculated for suppressors run in both dynamic recycle (n = 3) and stepped-legacy external water (n = 5) operation modes, respectively, as follows: 0.85 ± 0.3 and 0.18 ± 0.11 nmol (Li^+), 0.93 ± 0.37 and 0.16 ± 0.13 nmol (Na^+), and 1.24 ± 0.63 and 0.30 ± 0.20 nmol (K^+). We could not easily quantify the loss of NH_4^+ because it typically has a non-linear response over the calibration range.[44] However, NH_4^+ was observed to have systematically lower peak areas for calibration standards in dynamic recycled water compared to other suppression modes. For example, the peak areas in our 498 ng standards (mass on column) were 6.07, 3.72, and 1.87 μS·min for stepped-legacy recycle, stepped-legacy external, and dynamic recycle modes, respectively. A negative y-intercept was not observed in the suppressor when operated in stepped-legacy recycled water mode, meaning no loss of the inorganic cations was observed. As a result, all quantitative determinations of inorganic cations in the final optimized IC method use regression lines that are not forced through zero and the zero-point is retained when obtaining the form of the calibration curves.

3.3.2 Amine Standards

The same statistical procedures for calibrations were performed for the amine analyte suite. The results of the regression lines from the first approach showed R^2 values ranging from 0.890 to 0.990 and an RE % of -77 ~ +15. These R^2 values improved to 0.994 to 0.999 with an RE % of -

631 33 ~ +17 using the second approach. The best R^2 values of 0.998 to 0.999 as well as an RE % of -
632 13 ~ +20 were obtained using the third approach. Minimizing the residuals in the linear regression
633 for these analytes was best accomplished by excluding the zero-point from regression data sets
634 was unexpected. As a result, it was concluded here that the origin cannot be considered a valid
635 regression data point. This suggests it is a source of substantial error, meaning that analytes are
636 lost in the analytical system between injection and detection. Its inclusion is clearly detrimental to
637 achieving acceptable accuracy for quantitative analysis. A statistical test of standard error of the
638 intercept supported retaining the y-intercept in the resulting calibration curves, the same as was
639 found for the inorganic cations. The loss of amines can likewise be calculated from the x-intercept
640 of the linear regression in all three suppressor modes (n = 3 dynamic recycle and stepped-legacy
641 external water, n = 1 stepped-legacy recycle). The loss amounts were between 0.16 – 0.46 nmol
642 (dynamic recycle), 0.03 – 0.37 nmol (stepped-legacy recycle), and 0.13 – 0.32 nmol (stepped-
643 legacy external water). The loss of analytes can occur from damage accumulated in the resin of
644 the suppressor, making the ion-exchange function compromised.

645 Analyte loss was higher in dynamic compared to stepped-legacy suppressor modes for both
646 inorganic cations and amines. The loss of analytes from the suppressor was found to potentially
647 be associated with high current applied in dynamic mode, leading to over-suppression of the eluent
648 and analytes. For example, in one batch of analyses, an ideal current of 52 mA was automatically
649 calculated by the Chromeleon software for an eluent concentration of 8 mM MSA; meanwhile the
650 result of the recommended calculation is 30 mA (E1). In contrast to both of these values, on the
651 first injection in dynamic mode it was observed that the suppressor had an applied current of 110
652 mA, 2-3 times that required, and this declined to 80 mA over the subsequent injection of 36 more
653 samples; a value still well above either the ideal one or that obtained by E1. The suppressor current
654 operating at more than double the ideal value for the highest eluent concentration will affect the
655 functionality and lifetime of the suppressor. As a result, the use of dynamic mode for gradient
656 separations was found to be highly damaging to suppressor integrity and we used this option
657 minimally in order to obtain the comparisons throughout this work.

658 We also observed amine loss in stepped-legacy mode with recycled water, but without any
659 detectable loss of inorganic cations. In stepped-legacy external water mode, both the inorganic
660 cations and amines were found to have a similar magnitude of analyte loss, but the longest
661 suppressor lifetime. Overall, from this comprehensive assessment of all possible suppressor

operation modes, we have determined that the effect of analyte losses on the linear fitting of calibration curves needs to be considered in any cation gradient separations. By optimizing the functionality of the suppressor, we identified a preferred suppression mode: stepped-legacy external water; this allowed the calibration approach to also be defined. Henceforth, all the amine linear regressions used for quantitation are not forced through zero and the zero-point is excluded from the calibration curves, based on the IC method performance determinations presented in the following section.

3.4 Accuracy, Precision, and Limits with Different Suppression Modes

3.4.1 Inorganic Cation Standards

Accuracy and precision improvements for inorganic cations is the most notable driver of our suppressor operation selection, which is stepped-legacy external water mode. This is particularly true when compared to the limitations reported in prior calibration analyses of inorganic cations where the instrumentation all used eluent generation and legacy recycled water mode.[44,48] Accuracy, precision, and LOD of inorganic cations were measured in three different suppressor modes; results of our preferred method using stepped-legacy external water are presented in the SI (Table S4). Inorganic cations had measured accuracies of 83% to 99% in dynamic recycle, 87% to 99% in stepped-legacy recycle, and 95% to 99% in stepped-legacy external water, with precisions of ± 14%, ± 13%, and ± 8%, respectively. The divalent cation analytes Mg^{2+} and Ca^{2+} were not possible to detect after running a few (~20) samples in dynamic recycle mode, ~100 samples in stepped-legacy recycle mode, and ~300 samples in stepped-legacy external water when utilizing the optimized gradient elution conditions necessary to separate the target suite of atmospherically relevant alkylamines. Inorganic cations were found to have lower LODs in stepped-legacy mode compared to dynamic, with the lowest LODs for the optimized separation obtained in stepped-legacy recycled water. For example, independent of injection volume, NH_4^+ was found to have a LOD of 0.99 ± 0.72 nmol (dynamic recycle), 0.07 ± 0.05 nmol (stepped-legacy recycle), and 0.17 ± 0.12 nmol (stepped-legacy external water). These findings are generally consistent with the trend and relative magnitude of losses observed from the suppressor in the preceding section. Inorganic cation analysis demonstrated the highest accuracy and precision with the suppressor operated under stepped-legacy external water mode, with the added advantage of greater robustness in

detecting and quantifying Mg^{2+} and Ca^{2+}. Overall, there is improvement in IC separation method performance for this analyte mixture.

3.4.2 Amine Standards

Amine standards in DIW were also analyzed for accuracy and precision with suppressors in dynamic recycle and stepped-legacy separation modes with two different water supplies: recycle and external (Fig. 6). Comprehensive metrics on the performance of the stepped-legacy external water suppressor mode for amines are provided in Table S4. Amine standards were found to have the highest sensitivities when using stepped-legacy mode with recycled water, followed by external water. However, the suppressor had a shorter lifetime prior to critical failure when using recycled (~2 months) versus external water (~6 months). The lowest sensitivities observed in this work arise from operating the suppressor in dynamic recycle mode, probably due to analyte loss within the device, which was also associated with the shortest device lifetime (≤2 months).

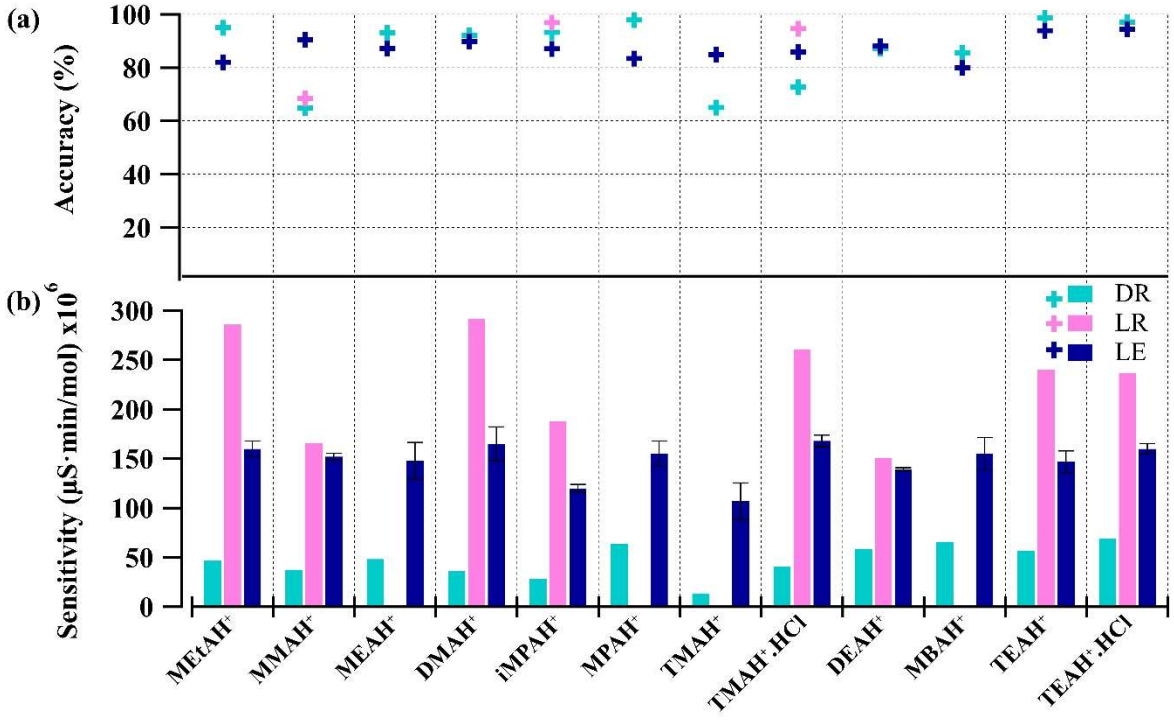

Fig. 6 (a) Accuracy and (b) sensitivity and calibration precision of alkyl amines for three different suppressor modes: dynamic (D) with recycled (R) water, stepped-legacy (L) with recycled water, and legacy with external (E) water. Replicates were only performed for LE (n = 3), while the other two (DR and LR) were only measured once as the devices failed quickly due to damage accumulated by the suppressors.

712 Accuracy of the method when operating the suppressor under dynamic mode with recycled water
713 was performed exclusively with freshly prepared standards. The accuracy of all amine standards
714 was calculated to be within 65% ~ 99% and precision was ± 14% when using dynamic recycled
715 water mode. Instrumental LODs were calculated for all of the target amines with an average of
716 1.51 nmol per injection (range: MBA = 0.26 ~ TEA = 5.61 nmol). Systematic amine calibrations
717 showed low sensitivities and rapid loss of detection for Mg^{2+} and Ca^{+2} in dynamic recycled mode
718 (Table S4). The suppressor was changed from dynamic to stepped-legacy mode while keeping the
719 water recycled. This was done to improve sensitivity, LODs, and duration of detection of Mg^{2+}
720 and Ca^{2+} peaks in a gradient method (see Section 3.5). The accuracy of freshly made standards
721 were only assessed using the amine mixture of MMA, iMPA, and TMA.HCl which were within
722 68% ~ 97% under stepped-legacy recycled water (Fig. 6a). This suite was selected as the analyte
723 retention times span the gradient. Monomethylamine did not show any accuracy improvement
724 when compared to the dynamic-recycle mode; however, the accuracy of the TMA.HCl improved
725 by 22 %. The precision was measured using the additional analytes MEtA, DMA, DEA, and TEA,
726 with values of ±15 % and a mean LOD of 0.44 nmol (range: MEtA = 0.08 ~ TEA = 1.87 nmol).
727 Overall, the result of standard analyses showed higher sensitivity for the amine suite, with lower
728 LODs, and it was possible to detect Mg^{2+} and Ca^{2+} peaks in ~100 samples. However, the suppressor
729 also critically failed in this mode when conducting gradient separations after two months and this
730 mode of operation did not improve suppressor lifetime compared to that of dynamic recycled
731 mode. Lastly, the water supply of the suppressor in stepped-legacy mode was switched to an
732 external water supply over recycling eluent from the detector. In this method, the accuracy of all
733 amine standards was much improved to a range spanning 80 % to 94 %, with MMA and TMA
734 particularly benefiting. The precision was calculated to be ±13 %, a marginal improvement, and
735 the calculated mean LOD as 0.64 nmol (range: MEtA & MBA = 0.13 ~ TEA = 3.41 nmol), a
736 marginal decline. In conclusion, the quantification of alkyl amines showed the highest accuracy
737 when using the stepped-legacy external water mode with a commensurate longer suppressor
738 lifetime, at the sacrifice of some sensitivity (Fig. 6). Improvement of both precision and accuracy
739 are observed under stepped-legacy external (Table S4) over the previous amine quantitative
740 analysis reported by Place *et. al.*[48] which was performed using legacy recycled water suppression.
741 The external water set up additionally reduces the accumulation of exchange materials that can
742 bleed from the column and/or formation of low solubility Mg^{2+} and Ca^{2+} hydroxide salts. This

allows these divalent cations to be detected in ~300 samples while simultaneously increasing the suppressor lifetime to six months before critical failure when conducting gradient separations.

3.5 Enhancement of Gradient Cation-Exchange Analysis by Suppression Mode Optimization

Quantifying amines in real samples is achieved using the highest IC method performance attainable with the optimum suppressor function and longest lifetime. Suppressor operation must be consistent to obtain sufficient robustness in the developed methodology. To achieve such optimization, cation calibration standards were analyzed using the three different modes of modern electrolytic suppressors and various cleaning procedures. Quantitative analysis of inorganic cations and amines standards were first explored with suppression under dynamic recycle water mode. In this setup, water is reused from the suppressed eluent post-detection for continuous regeneration of OH^- and H_3O^+ (Fig. 1). Cation calibrations had the lowest sensitivities, loss of monovalent inorganic cations (Li^+, Na^+, K^+, and NH_4^+) and alkylamines, and the loss of the capability to detect divalent cations Mg^{2+} and Ca^{2+} during gradient elution conditions. There are several potential explanations for this, where they could be occurring simultaneously or in isolation, depending on the suppression mode. First, if there is extra current provided in dynamic mode, this could lead to over-suppression which would produce an excess amount of OH^- compared to that required to neutralize the H_3O^+ competing ion. This excess OH^- could lead to the formation of Mg^{2+} and Ca^{2+} precipitates as highly insoluble hydroxide salts. Excess current can also generate excess heat, leading to the degradation of the anion exchange material, shortening the suppressor lifetime, which results in critical failure. Lastly, the exchange material of the analytical column may be bleeding into the suppressor resin and accumulate there over time, which can facilitate more rapid degradation, in addition to retaining divalent ions irreversibly. The performance of the prior line of resin-based suppressors, the cation electrolytically regenerated suppressor (Dionex CERS 500, 4 mm, P/N: 082542), was previously noted to be compromised by these same lost capabilities in detecting Mg^{2+} and Ca^{2+} when performing gradient cation separations.[48] Therefore, a variety of methods were tested in this work to formulate effective ways to prevent suppressor-related instrument sensitivity losses and increased LODs: acid (MSA) and base (NaOH) washes, changing from dynamic to stepped-legacy water recycle mode, oxalic acid wash, and changing regenerant water from recycled via the detector to an external water supply (see Section S6 for details). The best outcomes were obtained when we paired stepped-legacy

suppression mode with use of external water. No cleanups were required, and the system retained a high sensitivity for all analytes, while detecting Ca^{2+} and Mg^{2+} ions in ~300 samples, and resulted in the longest suppressor lifetime of 6 months before critical failure when performing gradient separations. The only way determined to retain Ca^{2+} and Mg^{2+} quantitative capabilities across thousands of analyses with this stationary phase and suppressor combination was through the use of isocratic separations with an MSA concentration of 8 mM and a flow rate of 1 mL min^{-1}, with a suppressor current of 24 mA and operation in legacy external water mode.

3.6 Comparison of Optimized Method to Previous Amine Separations

Ion chromatographic methods utilizing gradients of H_3O^+ to facilitate separations of mixtures of common inorganic cations and alkylamines have been developed over the past decade using several different cation-exchange columns from Dionex (now ThermoScientific): CS12A (8.5 μm), CS17 (7 μm), CS19 (5.5 μm), and CS19 (4 μm). Methanesulfonic acid gradient programs were used on the CS12A and CS17 cation-exchange columns at 30 °C with the cation self-regenerating suppressor (CSRS 300) under legacy recycle mode.[44] These methods obtained good resolution and reproducibility but the coelution of NH_4^+/$MMAH^+$/$MEAH^+$ occurred on CS12A, along with the coelution of $DEAH^+$/$TMAH^+$ on both columns. Five years later, this method was improved to analyze nine alkylamines with successful separation of $DEAH^+$/$TMAH^+$ using the CS19 (5.5 μm) column chemistry by increasing the separation temperature to 55 °C, which was paired with a cation electrolytically regenerated suppressor (CERS 500) operated using legacy recycle mode.[48] In the present work, the IC method development advances to analyze ten alkylamines by improving the selectivity of $MEtAH^+$ using the CS19 (4 μm) column at 55 °C with cation dynamically regenerated suppressor (CDRS 600) under three different water modes: dynamic recycle, stepped-legacy recycle, and stepped-legacy external.

Three different suppressors were used in these methods: CSRS 300, CERS 500, and CDRS 600; the main differences being in the material of the ion-exchanger in the eluent channel. All were applied to gradient separations. Gasketed screen is used in the CSRS 300 as opposed to the resin beds in CERS 500 and CDRS 600. The CSRS 300 and CERS 500 can only be operated in legacy mode by setting the electric current, ideally using E1. The CDRS 600 has an updated resin composition to enable operation in dynamic mode, in addition to the traditional legacy mode, without setting the electric current requirement, but instead applying a constant voltage that should

theoretically be current-responsive to changes in eluent conductivity. The highest sensitivities of mixed inorganic cations were observed when using the CERS 500 operated in legacy recycle mode by Place *et al.*(Fig. S7).[48] In the present study, the lowest sensitivities were observed for the CDRS 600 in dynamic recycle mode with total loss of detection for Mg^{2+} and Ca^{2+} analytes. The suppressor did not work as expected to automatically adjust the current based on the eluent ion concentration and over-suppression at eluent concentrations of 1 mM MSA were often observed. Sensitivity improvement in detection of alkylamines was observed in the stepped-legacy suppressor mode of the present work compared to the prior work of Place *et al.* and VandenBoer *et al.*, where CS19 and CS17 stationary phase chemistries were used, respectively (Fig. 7).[44,48] Even though $MMAH^+$ and $MEAH^+$ showed high separation efficiency (and sensitivities as a result) when separated using the CS12A, they coeluted with NH_4^+. Since the latter is ubiquitous in atmospheric samples, the amines would not be possible to detect as unknown analytes in real samples subject to conductivity detection.

Overall, in the current study, we could detect and quantify the ten most abundant alkylamines and six inorganic cations with the improvement of separation efficiency and resolution, such as $DEAH^+$ and $TMAH^+$ by using the new 4 μm stationary phase. Accuracy and precision improvement were achieved mainly in NH_4^+ and TMA.HCl, in addition to identifying optimum suppression function for the CDRS 600 through stepped-legacy external water mode in gradient separations. This overcomes the challenges of losing analytes and exhibits the greatest longevity of electrolytically regenerated resin-based suppressor. This highly selective developed IC-CD method allowed us to separate and quantify inorganic cations in addition to a large suite of amines expected to be present in real samples of atmospheric aerosol and as gases. We demonstrate this through the analysis of size-resolved marine aerosol samples and indoor gas samples.

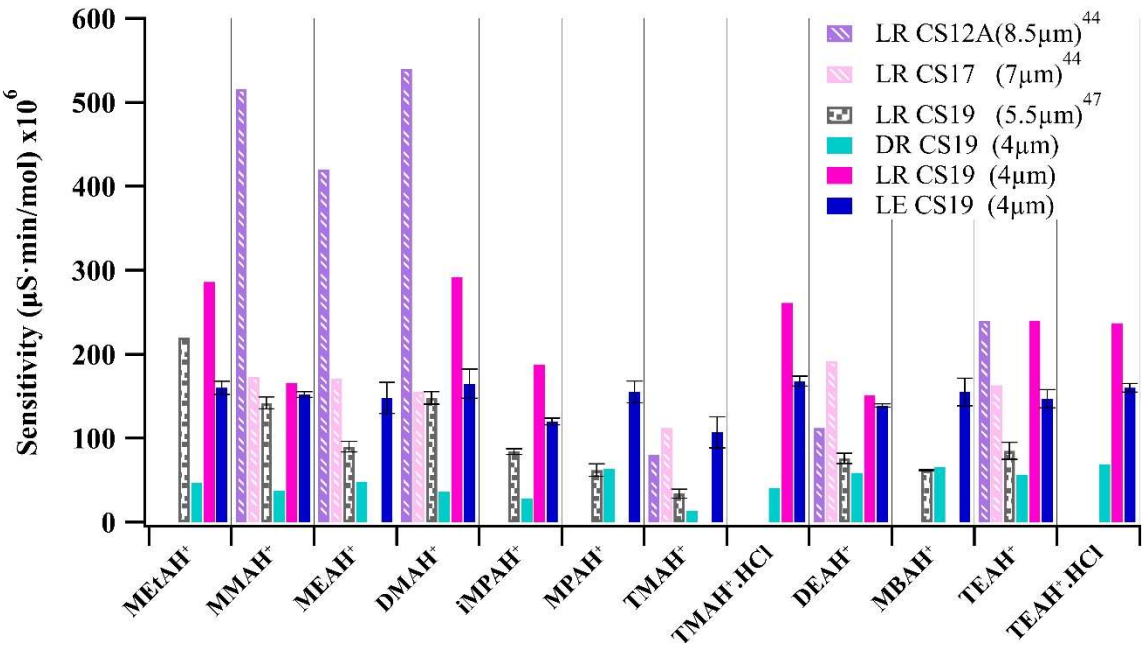

Fig. 7 Sensitivity of alkylamines by using different cation-exchange columns and suppressors over a decade (legacy or stepped-legacy (L) and dynamic (D) modes, with recycled (R) or externally (E) provided water). The analyte separation and suppression performed by CS12A (8.5 μm) and CS17 (7 μm) analytical columns with a CSRS 300 operated in LR were made by VandenBoer *et al.*[44]; a CS19 (5.5 μm) analytical column with a CERS 500 operated in LR by Place *et al.*[48]; and CS19 (4 μm) analytical column with a CDRS 600 with DR, LR, and LE determined in this work.

3.7 Quantifying NH_4^+ and Alkylamines in Size-Resolved Marine Aerosols

Sample analysis of size-resolved aerosol was conducted at the beginning of our IC method development, as many of the reported issues herein were not yet identified. Nonetheless, sample analytes were separated with the mobile phase flow rate of 1.25 mL min^{-1} and a column temperature of 35 °C. The eluent gradient program was slightly different from the optimized version that we report here. This method added 5 more minutes in the exponential ramp from 4 to 8 mM MSA and used a longer equilibration time for the 1 mM MSA (5 vs 9 minutes). The suppressor was operated using dynamic mode with recycled water to analyze these samples. Due to time constraints, they were immediately analyzed after extraction and insufficient volume remained for reanalysis with the optimized method obtained years later. Despite the conditions not being the best performing obtained, amines were ubiquitously detected in all aerosol samples and were possible to quantify, with several new species detected for the first time.

First, more generally, the molar ratio of the sum of aminium ions to ammonium ranged from 0.02 to 0.2, consistent with the emerging understanding of the importance of amines in marine

particle composition. Alkylamines have been detected in marine aerosols and have been implied to make key contributions to new particle formation and aerosol growth.[70–73] The size-resolved aerosol composition from our MOUDI samples were categorized in a bulk approach based on larger bins of particle diameter: 0.1–1 μm (fine mode) and 1–100 μm (coarse mode). The results of the fine mode show that cation molar quantities were in excess of anions in these marine aerosol water soluble ion observations, with a charge balance ratio (Σ+/Σ-) of 1.58 (Fig. 8a). Di Lorenzo *et al.*[74] observed cationic excess with (Σ+/Σ-) > 2 in the composition of size-resolved aerosols from aged biomass burning samples that transited the coastal marine atmosphere prior to collection. The excess of cations in this prior work was suggested to be due to the formation of stable salts of reduced nitrogen and small organic acids or carboxylate functional groups found ubiquitously in oxidized secondary organic aerosol.[75] The reactive uptake of ammonia and amines by carbonyls was another hypothesized pathway, based on findings reported from a number of lab studies.[19,76] A similar ion imbalance has also been observed as an emerging trend in the chemical composition analysis of continentally-originating cloud water at Whiteface Mountain; where an increasing trend in (Σ+/Σ-) was also associated with missing anion measurements in those samples.[77]

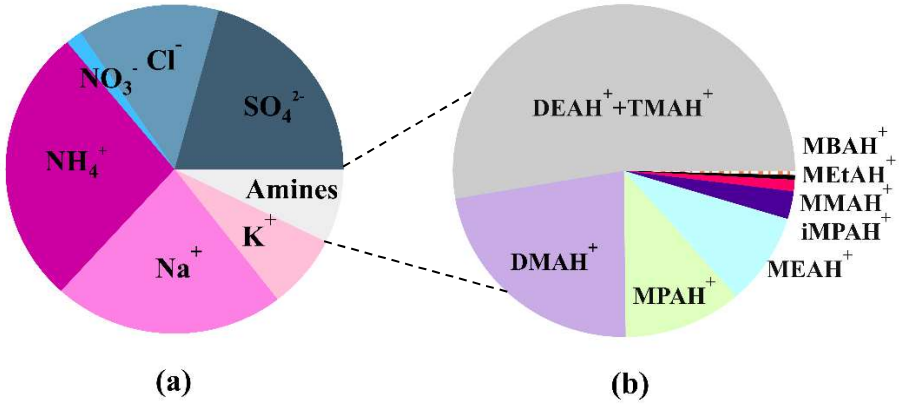

Fig. 8 Sum of total equivalent ionic loading of (a) cations, and (b) alkylamines in fine mode aerosol. The equivalent ionic loading were 23 and 4 neq m^{-3} for NH_4^+ and amines, respectively, which were quantified in this MOUDI sample from the coast of Eastern Canada.

Two amines were unresolved in this initial analysis: $DEAH^+$ and $TMAH^+$ because the column temperature was only 35 °C, which limited the stationary phase selectivity. Compared to the other quantified amines, the analysis of $DEAH^+$ + $TMAH^+$ was found to have the highest equivalent ionic loading estimated at 2.29 neq m^{-3} (Fig. 8b). Average calibration slopes and

molecular weights (MW) of $DEAH^+$ and $TMAH^+$ were used to estimate the concentration of the coeluting $DEAH^+$ and $TMAH^+$. Unfortunately, by the time our final optimized method was achieved, the limited sample volume remaining was insufficient for reanalysis, and they had been in storage for a substantial period of time (> 1 year). Diethylamine (DEA) is one of the most abundant amines detected in marine atmospheres and aerosols, with known biogenic sources,[78] making it the more likely contributor to our observed peak, which would decrease the 2.29 neq m^{-3} by a factor of 1.2 (if using its calibrated sensitivity and MW) to 1.91 neq m^{-3}. In a gas-particle partitioning framework, DEA can form more stable salts than other methyl and ethyl amines (mono-, di-, and tri-) due to its high basicity,[78] such as in its thermodynamically favorable reaction with HNO_3,[39] in addition to the stability of diethylaminium nitrate salt toward oxidation.[16] However, trimethylamine (TMA) is also an abundant and common amine in the atmosphere; it has mainly been found to be emitted from animal husbandry, biomass burning, as well as biological degradation of osmoregulatory compounds such as glycine betaine (GBT), trimethylamine N-oxide (TMAO), and choline in marine organisms with global emissions estimated at 169 ± 33 Gg N a^{-1}.[5,79,80] If TMA were the sole source of our observation, the 2.29 neq m^{-3} would increase by a factor of 1.2 to 2.75 neq m^{-3}. In addition, three new amines: MPA (0.49 neq m^{-3}), iMPA (0.12 neq m^{-3}), and MBA (0.02 neq m^{-3}) were detected and quantified in these MOUDI samples, which have not been reported in prior studies of marine particles. Ion mass concentrations of two MOUDI samples show the differences between amine mass loadings in coastal marine and anthropogenically influenced harbour air (Figs. 9 and S8). The summed amine equivalent ionic loadings are higher in the marine air than in the harbour air with value of 1.55 and 0.76 neq m^{-3}, respectively. The advantage of applying our highly selective IC method is it can quantify a large suite of amines in marine aerosol samples. Because this method resolved all the amine analytes from the highly abundant sodium in these samples, we were able to identify several new species that have not been previously reported. Therefore, application of this improved IC method can inform future field studies about reduced nitrogen basic species of interest and their importance in Earth's atmosphere. Those results can then inform laboratory studies to better understand the roles physical, chemical, and biological processes have on the composition of aerosol, or in the exchange of gases and particles across the air-sea interface.

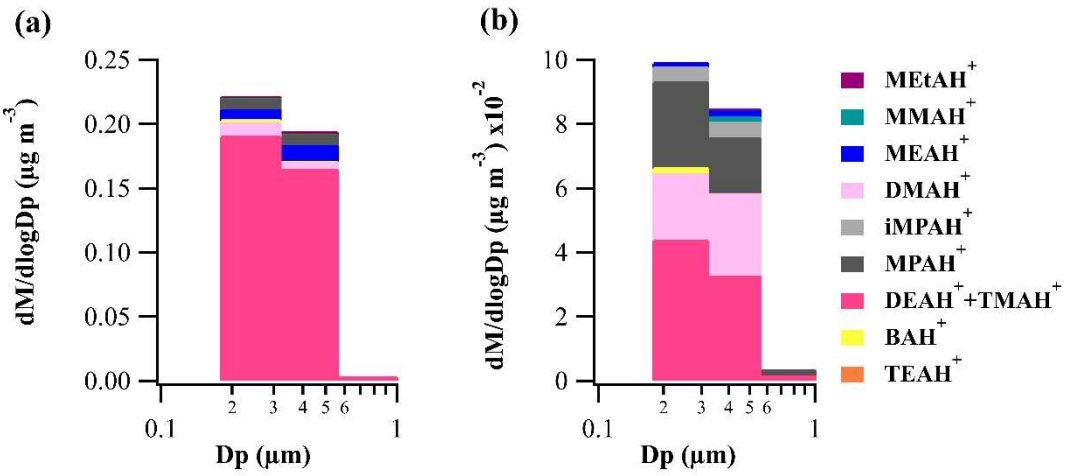

Fig. 9. Ion mass loadings of MOUDI samples is shown only in fine mode (particle diameter less than 0.1 µm) in (a) marine air from 15/09/2018 to 16/09/2018, and (b) Halifax harbour air from 18/09/2018 to 19/09/2018 on the Atlantic coast of Nova Scotia, Canada (Fig. S8). The amine mass loading in the coarse mode is not depicted because levels were below detection limits.

3.8 Indoor Measurement of NH_3 and Alkylamines

Quantification of indoor NH_3 and amines from passive sample collection was performed with the optimized gradient method at 55 °C and stepped-legacy external water suppression. Ammonia was the dominant basic indoor compound during the New Home Air Quality Study (NHAQS), with a mean mixing ratio of 25 ± 15 ppbv, ranging from 4 – 79 ppbv through the different time periods of occupancy. Unfortunately, amine levels were below the instrumental LODs, and we could not detect and quantify them in either indoor or outdoor samples. The maximum mixing ratios for detectable amines is between 0.34 ppbv for MMA which we detect the most sensitively and 10.50 ppbv for TEA which is the least sensitive for a sampling time of 1 day. These limits decrease to 0.08 ppbv for MMA and 2.59 ppbv for TEA when the sampling time is extended to 5 days. The upper limits for the mixing ratios of the full analyte suite detectable by our optimized IC method are presented in Table S5.

The concentration of NH_3 in previous studies ranged between 8 – 44 ppbv in a variety of residential buildings (Fig. 10).[81–84] Ampollini *et al.*[29] measured a mean mixing ratio of 32 ppbv in an unoccupied test house with increasing maximum concentrations of NH_3 during different activities, including cooking meat (130 ppbv), cleaning with ammonia-based products (1592 ppbv), and high-occupancy events (99 ppbv). Indoor measurements of amines have been performed in a few studies, and primarily aromatic amines were reported in a tobacco smoking

environment .[85–87] Akyüz quantified alkylamines in indoor (smoking and non-smoking areas) and outdoor air samples during the summer and winter months at six sampling sites in Turkey. Seasonal mean concentrations of MMA, DMA, MEA, DEA, MPA, and MBA were determined at mass loading levels of ng m^{-3} which are on the same order as pptv mixing ratios.[88] Our IC method can detect and quantify the ten most abundant atmospheric alkylamines, yet LODs for 24 hr and 5 day integrated sampling when assuming the same sampling rate as for NH_3 range from 0.14 – 30 µg m^{-3}, which are equivalent to mixing ratios on the order of ppbv, so this passive sampling technique is more applicable for detecting or quantifying amines from emission sources. Our findings here show that there are not strong sources of alkyl amines in newly built Canadian homes and that they were also not located near any strong outdoor point sources.

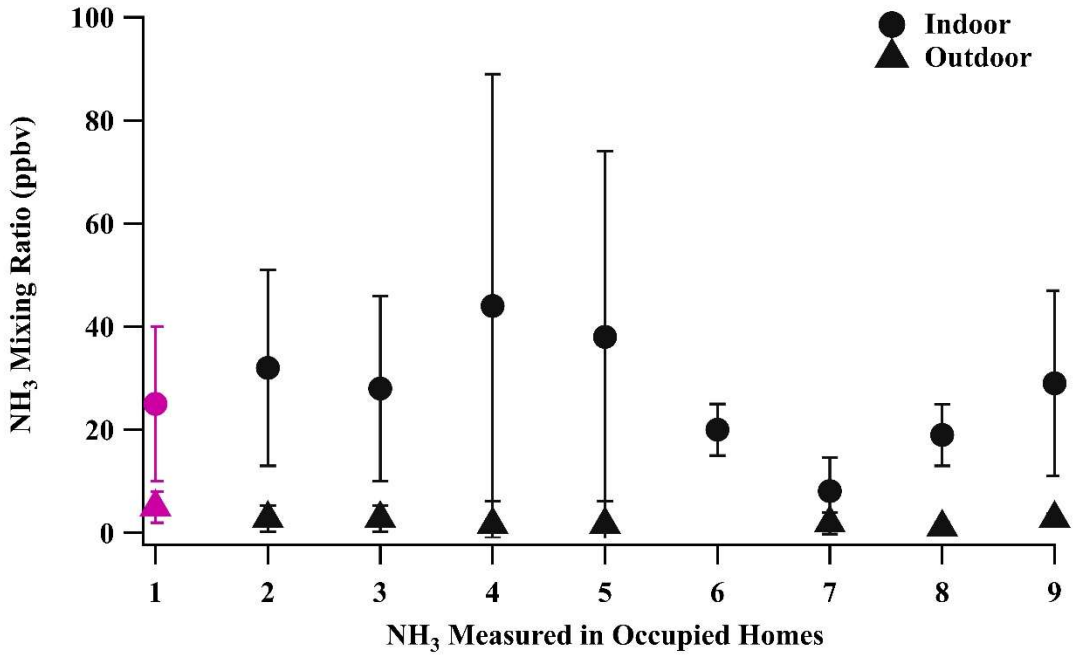

Fig. 10 Mixing ratios of NH_3 from NHAQS compared to previous studies in different occupied residential buildings: NHAQS (1, this work), Leaderer *et al.* (2, summer; AC ON),[81] (3, summer; AC OFF),[81] (4, winter; kerosene heater ON),[81] (5, winter; kerosene heater OFF),[81] Spengler *et al.* (6)[82], Brauer *et al.* (7, summer)[83], (8, winter)[83], and Li and Harrison (9)[84].

Mixing ratios of NH_3 decreased in the majority of homes after occupancy in the NHAQS (Fig. 11a), potentially due to either reduction in emissions from new building materials or an increase in surface area from occupancy to which it can partition. When occupants moved in, the surface/volume increased through the addition of furniture, personal materials, and the occupants into the houses. This amplifies the emerging recognition that surface interactions and their

influence on the chemical composition of indoor air is important.[89,90] In a case study, the ammonia mixing ratio in one home decreased significantly from 79 ppbv pre-occupancy to 18 ppbv during the first year of occupancy (Fig. 11b). The simultaneously measured outdoor mean mixing ratio of NH_3 was 4 ± 2 ppbv. The indoor to the outdoor ratio of NH_3 was typically greater than unity in all 18 houses, consistent with the known indoor sources of NH_3. A more detailed analysis on NHAQS indoor NH_3 is beyond the scope of this work as sample collections from a larger number of homes is ongoing and will be the subject of future work.

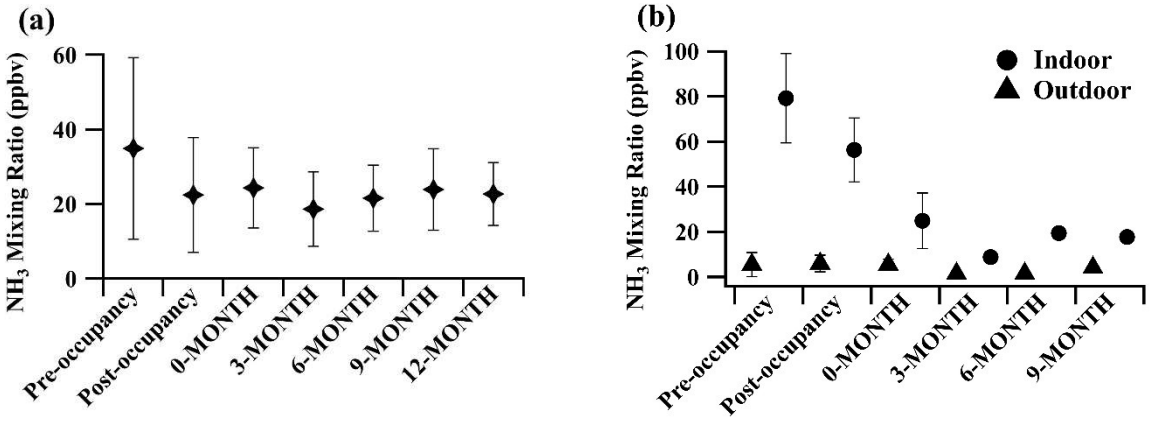

Fig. 11. NHAQS observations of (a) average indoor mixing ratios of NH_3 (±1σ) from pre-occupancy through the first-year occupancy in 18 houses (b) outdoor and indoor mixing ratios of NH_3 (±1σ) from pre-occupancy to 9-MONTH in the case study home.

4. Conclusions

The ion-chromatographic method was developed with high selectivity and separation efficiency to quantify six inorganic cations and ten most abundant alkylamines found in the atmosphere, including MEtA, which was not measured in previous reports. This method was optimized in separation efficiency and resolution of cations using a smaller particle size of 4 μm on a CS19 cation-exchange column and a resin-based suppressor operated in stepped-legacy external water mode. The stability of amine standards was not improved overtime by decreasing the pH and fixing the ionized state of standards as hydrochloride salts; amine standards must be made freshly from stock solutions from the primary standards prior to quantitative analysis in DIW to achieve the highest instrument reproducibility and method accuracy. TMA standards have been previously reported for high variability between days due to its high volatility; in this study, we found that a

freshly made stock solution of its hydrochloride salt improves IC method performance and recommend the same for quantitation of TEA. Despite losing analytes in the modern anion-exchange resin suppressors operating on a gradient elution program, the most accurate calibration curves of cation standards were obtained using regression lines that are not forced through zero. For inorganic cations, the zero-point was retained, whereas for amines, the zero-point was excluded. Analysis of calibration of inorganic cations and alkylamines was then optimized using a suppressor operated with stepped-legacy external water to obtain higher accuracy and precision, while also detecting the divalent cations Mg^{2+} and Ca^{2+} with the longest suppressor lifetime prior to critical failure.

Overall, this highly selective developed IC-CD method allowed us to separate and quantify inorganic cations and large suites of amines in real samples. The result from size-resolved aerosols suggests that NH_3 and amines are diverse and abundant in the marine environment; MPA, iMPA, and MBA were detected and quantified in these samples, which have not been reported before Therefore, more research will be required to understand the chemical composition of aerosol in the exchange of gases and particles across the air-sea interface. The result from NHAQS will be used to explore associations between homeowners' activities and observed NH_3 mixing ratios to better understand the controls on their emission sources, and to set initial upper limits on indoor amines. These estimates are important for ongoing regulate of NH_3 and amine emissions from new building materials that could lead to occupant exposure and subsequent health effects.

Author Contributions

Conceptualization, data analysis, editing manuscript and funding: TV. Methodology, formal analysis, validation, investigation, and writing the original draft and editing: LS.

Conflicts of interest

There are no conflicts to declare.

Acknowledgements

This work was funded by the Alfred P. Sloan Foundation Chemistry of Indoor Environments (CIE) Program (Awards G-2018-11062, G-2018-11051), and by the National Science and Engineering Research Council of Canada (NSERC) Discovery Grants and Discovery Launch Supplement

(RGPIN-2020-06166 and DGECR-2020-00186). We acknowledge Wood Group PLC for collecting size-resolved MOUDI aerosol samples from the Coastal Fog study. We thank Health Canada for deploying passive samplers in the NHAQS which is funded under the Addressing Air Pollution Horizontal Initiative. We would like to acknowledge H. You, M. MacNeill, J. Moore, and K. Van Ryswyk for their valuable contributions in arranging and collecting NHAQS samples for this study. LS was supported by Harold I. Schiff and Charles Hantho awards in Atmospheric Chemistry, Ontario Graduate Scholarship, and an Enbridge Graduate Award. Finally, we would like to thank C. Young for providing valuable feedback on the manuscript.

References

1 X. Ge, A. S. Wexler and S. L. Clegg, Atmospheric amines - Part I. A review, *Atmos. Environ.*, 2011, **45**, 524–546.

2 X. C. Wang and C. Lee, Sources and distribution of aliphatic amines in salt marsh sediment, *Org. Geochem.*, 1994, **22**, 1005–1021.

3 D. H. Scharffe, J. M. Lobert, P. J. Crutzen and W. M. Hao, Importance of Biomass Burning in the Atmospheric Budgets of Nitrogen-Containing Gases, *Nature*, 1990, **346**, 552–554.

4 F. Toribio, E. Moyano, L. Puignou and M. T. Galceran, Determination of heterocyclic aromatic amines in meat extracts by liquid chromatography-ion-trap atmospheric pressure chemical ionization mass spectrometry, *J. Chromatogr. A*, 2000, **869**, 307–317.

5 G. W. Schade and P. J. Crutzen, Emission of aliphatic amines from animal husbandry and their reactions: Potential source of N2O and HCN, *J. Atmos. Chem.*, 1995, **22**, 319–346.

6 D. H. O'Neill and V. R. Phillips, A review of the control of odour nuisance from livestock buildings: Part 3, properties of the odorous substances which have been identified in livestock wastes or in the air around them, *J. Agric. Eng. Res.*, 1992, **53**, 23–50.

7 I. Schmeltz and D. Hoffmann, Nitrogen-Containing Compounds in Tobacco and Tobacco Smoke, *Chem. Rev.*, 1977, **77**, 295–311.

8 G. W. Harris, R. Atkinson and J. N. Pitts, Kinetics of the reactions of the OH radical with hydrazine and methylhydrazine, *J. Phys. Chem.*, 1979, **83**, 2557–2559.

9 N. R. Passant, P. J. Swannell and N. Ginson, E M I S S I O N S O F V O L A T I L E O R G A N I C C O M P O U N D S (VOCs) FROM THE FOOD AND DRINK INDUSTRIES OF THE EUROPEAN COMMUNITY, 1993, **27**, 2555–2566.

10 W. R. Pierson and W. W. Brachaczek, Emissions of Ammonia and Amines from Vehicles on the Road, *Environ. Sci. Technol.*, 1983, **17**, 757–760.

11 S. M. Calderón, N. D. Poor and S. W. Campbell, Estimation of the particle and gas scavenging contributions to wet deposition of organic nitrogen, *Atmos. Environ.*, 2007, **41**, 4281–4290.

12 L. J. Carpenter, S. D. Archer and R. Beale, Ocean-atmosphere trace gas exchange, *Chem. Soc. Rev.*, 2012, **41**, 6473–6506.

13 X. Ge, A. S. Wexler and S. L. Clegg, Atmospheric amines – Part I. A review, *Atmos. Environ.*, 2011, **45**, 524–546.

14 L. Grönberg, P. Lövkvist and J. Å. Jönsson, Determination of aliphatic amines in air by membrane enrichment directly coupled to a gas chromatograph, *Chromatographia*, 1992, **33**, 77–82.

15 T. Bergman, A. Laaksonen, H. Korhonen, J. Malila, E. M. Dunne, T. Mielonen, K. E. J. Lehtinen, T. Kühn, A. Arola and H. Kokkola, Geographical and diurnal features of amine-enhanced boundary layer nucleation, *J. Geophys. Res.*, 2015, **120**, 9606–9624.

16 A. Sorooshian, S. M. Murphy, S. Hersey, H. Gates, L. T. Padro, A. Nenes, F. J. Brechtel, H. Jonsson, R. C. Flagan and J. H. Seinfeld, Comprehensive airborne characterization of aerosol from a major bovine source, *Atmos. Chem. Phys.*, 2008, **8**, 5489–5520.

17 J. F. Pankow, Gas/particle partitioning of neutral and ionizing compounds to single and multi-phase aerosol particles. 1. Unified modeling framework, *Atmos. Environ.*, 2003, **37**, 3323–3333.

18 C. Qiu and R. Zhang, Multiphase chemistry of atmospheric amines, *Phys. Chem. Chem. Phys.*, 2013, **15**, 5738–5752.

19 D. O. De Haan, M. A. Toblert and J. L. Jimenez, Atmospheric condensed-phase reactions of glyoxal with methylamine, *Geophys. Res. Lett.*

20 V. R. Piers Forster, Changes in Atmospheric Constituents and in Radiative Forcing (IPCC 2007), *Change*, 2007, **30**, 129–234.

21 U. Lohmann and J. Feichter, Global indirect aerosol effects: a review, *Atmos. Chem. Phys.*, 2005, **5**, 715–737.

22 A. Van Neste and R. A. Duce, Methylamine in the marine atmosphere, 1987, **14**, 711–714.

23 K. G. McGregor and C. Anastasio, Chemistry of fog waters in California's Central Valley: 2. Photochemical transformations of amino acids and alkyl amines, *Atmos. Environ.*, 2001, **35**, 1091–1104.

24 P. Hou, S. Wu, J. L. McCarty and Y. Gao, Sensitivity of atmospheric aerosol scavenging to precipitation intensity and frequency in the context of global climate change, *Atmos. Chem. Phys.*, 2018, **18**, 8173–8182.

25 M. Mircea, S. Stefan and S. Fuzzi, Precipitation scavenging coefficient: Influence of measured aerosol and raindrop size distributions, *Atmos. Environ.*, 2000, **34**, 5161–5167.

26 N. E. Klepeis, W. C. Nelson, W. R. Ott, J. P. Robinson, A. M. Tsang, P. Switzer, J. V. Behar, S. C. Hern and W. H. Engelmann, The National Human Activity Pattern Survey (NHAPS): A resource for assessing exposure to environmental pollutants, *J. Expo. Anal. Environ. Epidemiol.*, 2001, **11**, 231–252.

27 M. Li, C. J. Weschler, G. Bekö, P. Wargocki, G. Lucic and J. Williams, Human Ammonia

Emission Rates under Various Indoor Environmental Conditions, *Environ. Sci. Technol.*, 2020, **54**, 5419–5428.

28 M. Hesta, G. P. J. Janssens, S. Millet and R. De Wilde, Prebiotics affect nutrient digestibility but not faecal ammonia in dogs fed increased dietary protein levels, *Br. J. Nutr.*, 2003, **90**, 1007.

29 L. Ampollini, E. F. Katz, S. Bourne, Y. Tian, A. Novoselac, A. H. Goldstein, G. Lucic, M. S. Waring and P. F. Decarlo, Observations and Contributions of Real-Time Indoor Ammonia Concentrations during HOMEChem, *Environ. Sci. Technol.*, 2019, **53**, 8591–8598.

30 R. E. Dodson, M. Nishioka, L. J. Standley, L. J. Perovich, J. G. Brody and R. A. Rudel, Endocrine disruptors and asthma-associated chemicals in consumer products., *Environ. Health Perspect.*, 2012, **120**, 935–43.

31 Z. Bai, Y. Dong, Z. Wang and T. Zhu, Emission of ammonia from indoor concrete wall and assessment of human exposure, *Environ. Int.*, 2006, **32**, 303–311.

32 W. W. Nazaroff and C. J. Weschler, Cleaning products and air fresheners: Exposure to primary and secondary air pollutants, *Atmos. Environ.*, 2004, **38**, 2841–2865.

33 B. Savonius, H. Keskinen, M. Tuppurainen and L. Kanerva, Occupational asthma caused by ethanolamines, *Allergy*, 1994, **49**, 877–881.

34 T. Wainright and L. Hall, gen trioxide (N2O3) and nitrogen tetroxide (N2O4) as it dissolves in water in the moist malt or in malt, 1986, **92**, 49–64.

35 K. A. Pratt, L. E. Hatch and K. A. Prather, Seasonal volatility dependence of ambient particle phase amines, *Environ. Sci. Technol.*, 2009, **43**, 5276–5281.

36 P. J. Silva and K. A. Prather, Interpretation of mass spectra from organic compounds in aerosol time-of-flight mass spectrometry, *Anal. Chem.*, 2000, **72**, 3553–3562.

37 J. N. Smith, K. C. Barsanti, H. R. Friedli, M. Ehn, M. Kulmala, D. R. Collins, J. H. Scheckman, B. J. Williams and P. H. McMurry, Observations of aminium salts in atmospheric nanoparticles and possible climatic implications, *Proc. Natl. Acad. Sci.*, 2010, **107**, 6634–6639.

38 F. L. Eisele, M. Chen, J. Zhao, C. Kuang, P. H. McMurry and J. N. Smith, Observation of neutral sulfuric acid-amine containing clusters in laboratory and ambient measurements, *Atmos. Chem. Phys.*, 2011, **11**, 10823–10836.

39 S. M. Murphy, A. Sorooshian, J. H. Kroll, N. L. Ng, P. Chhabra, C. Tong, J. D. Surratt and E. Knipping, Secondary aerosol formation from atmospheric reactions of aliphatic amines, *Atmos. Chem. Phys.*, 2007, 2313–2337.

40 L. Pan, J. M. Chong and J. Pawliszyn, Determination of amines in air and water using derivatization combined with solid-phase microextraction, *J. Chromatogr. A*, 1997, **773**, 249–260.

41 B. Sahasrabuddhey, A. Jain and K. K. Verma, Determination of ammonia and aliphatic

amines in environmental aqueous samples utilizing pre-column derivatization to their phenylthioureas and high performance liquid chromatography, *Analyst*, 1999, **124**, 1017–1021.

42 E. Dabek-Zlotorzynska and W. Maruszak, Determination of dimethylamine and other low-molecular-mass amines using capillary electrophoresis with laser-induced fluorescence detection, *J. Chromatogr. B Biomed. Appl.*, 1998, **714**, 77–85.

43 S. A. Bouyoucos, Determination of Ammonia and Methylamines in Aqueous Solutions by Ion Chromatography, *Anal. Chem.*, 1977, **49**, 401–403.

44 T. C. VandenBoer, M. Z. Markovic, A. Petroff, M. F. Czar, N. Borduas and J. G. Murphy, Ion chromatographic separation and quantitation of alkyl methylamines and ethylamines in atmospheric gas and particulate matter using preconcentration and suppressed conductivity detection, *J. Chromatogr. A*, 2012, **1252**, 74–83.

45 A. P. Sullivan, K. B. Benedict, C. M. Carrico, M. K. Dubey, B. A. Schichtel and J. L. Collett, A quantitative method to measure and speciate amines in ambient aerosol samples, *Atmosphere (Basel).*, 2020, **11**, 1–14.

46 M. L. Dawson, V. Perraud, A. Gomez, K. D. Arquero, M. J. Ezell and B. J. Finlayson-Pitts, Measurement of gas-phase ammonia and amines in air by collection onto an ion exchange resin and analysis by ion chromatography, *Atmos. Meas. Tech.*, 2014, **7**, 2733–2744.

47 R. J. Huang, W. B. Li, Y. R. Wang, Q. Y. Wang, W. T. Jia, K. F. Ho, J. J. Cao, G. H. Wang, X. Chen, I. Ei Haddad, Z. X. Zhuang, X. R. Wang, A. S. H. Prévôt, C. D. O'Dowd and T. Hoffmann, Determination of alkylamines in atmospheric aerosol particles: A comparison of gas chromatography-mass spectrometry and ion chromatography approaches, *Atmos. Meas. Tech.*, 2014, **7**, 2027–2035.

48 B. K. Place, A. T. Quilty, R. A. Di Lorenzo, S. E. Ziegler and T. C. VandenBoer, Quantitation of 11 alkylamines in atmospheric samples: Separating structural isomers by ion chromatography, *Atmos. Meas. Tech.*, 2017, **10**, 1061–1078.

49 T. Scientific, Dionex DRS 600 Suppressor Dionex ERS 500e Suppressor Dionex ERS 500 Carbonate Suppressor.

50 F. Raposo, Postprint of TrAC Trends in Analytical Chemistry Volume 77 , March 2016 , Pages 167-185 DOI : https://doi.org/10.1016/j.trac.2015.12.006 Evaluation of analytical calibration based on least-squares linear regression for instrumental techniques : A tutorial, 2016, **77**, 167–185.

51 S. L. R. Ellison, V. J. Barwick and T. J. Duguid Farrant, *Practical Statistics for the Analytical Scientist*, The Royal Society of Chemistry, UK, 2nd Editio., 2019, vol. 53.

52 J. G. Eisenhauer, Regression through the origin, *Teach. Stat.*, 2003, **25**, 76–80.

53 H. J. S. Fernando, I. Gultepe, C. Dorman, E. Pardyjak, Q. Wang, S. W. Hoch, D. Richter, E. Creegan, S. Gaberšek, T. Bullock, C. Hocut, R. Chang, D. Alappattu, R. Dimitrova, D. Flagg, A. Grachev, R. Krishnamurthy, D. K. Singh, I. Lozovatsky, B. Nagare, A. Sharma, S. Wagh, C. Wainwright, M. Wroblewski, R. Yamaguchi, S. Bardoel, R. S. Coppersmith, N. Chisholm, E. Gonzalez, N. Gunawardena, O. Hyde, T. Morrison, A. Olson, A. Perelet,

W. Perrie, S. Wang and B. Wauer, C-FOG life of coastal fog, *Bull. Am. Meteorol. Soc.*, 2021, **102**, E244–E272.

54 N. Chisholm, B. Nagare, C. Wainwright, E. Creegan, L. Salehpoor, T. C. VandenBoer, T. Bullock, B. Croft, G. Lesins, H. Osthoff, H. J. S. Fernando and R. Y. W. Chang, Characterizing Atmospheric Aerosols off the Atlantic Canadian Coast During C-FOG, *Boundary-Layer Meteorol.*, 2021, **181**, 345–364.

55 M. J. Roadman, J. R. Scudlark, J. J. Meisinger and W. J. Ullman, Validation of Ogawa passive samplers for the determination of gaseous ammonia concentrations in agricultural settings, *Atmos. Environ.*, 2003, **37**, 2317–2325.

56 J. S. Fritz and D. T. Gjerde, *Ion chromatography*, Wiley-VCH Verlag GmbH & Co. KGaA, Weinheim, Germany, 2009.

57 J. Weiss, *Handbook of ion chromatography*, Wiley-VCH Verlag GmbH & Co. KGaA, Weinheim, Germany, 2016.

58 S. J. Hawkes, Modernization of the van Deemter equation for chromatographic zone dispersion, *J. Chem. Educ.*, 1983, **60**, 393–398.

59 C. A. Pohl, J. R. Stillian and P. E. Jackson, Factors controlling ion-exchange selectivity in suppressed ion chromatography, *J. Chromatogr. A*, 1997, **789**, 29–41.

60 P. R. Haddad and P. E. Jackson, *Ion chromatography: principles and applications*, Elsevier, J. Chromatography library, New York, U.S.A, 1990.

61 J. Li and P. W. Carr, Effect of Temperature on the Thermodynamic Properties, Kinetic Performance, and Stability of Polybutadiene-Coated Zirconia, *Anal. Chem.*, 1997, **69**, 837–843.

62 S. T. Lee and S. V. Olesik, Comparison of Enhanced-Fluidity and Elevated-Temperature Mobile Phases in Reversed-Phase High-Performance Liquid Chromatography, *Anal. Chem.*, 1994, **66**, 4498–4506.

63 C. McNeff and P. W. Carr, Synthesis and Use of Quaternized Polyethylenimine-Coated Zirconia for High-Performance Anion-Exchange Chromatography, *Anal. Chem.*, 1995, **67**, 3886–3892.

64 G. Sheng, Y. Shen and M. L. Lee, Elevated Temperature Liquid Chromatography Using Reversed-Phase Packed Capillary Columns, *J. Microcolumn Sep.*, 1997, **9**, 63–72.

65 P. Hatsis and C. A. Lucy, Evaluation of column temperature as a means to alter selectivity in the cation exchange separation of alkali metals, alkaline earth metals and amines, *Analyst*, 2001, **126**, 2113–2118.

66 D. A. Skoog, F. J. Holler and S. R. Crouch, *Principles of instrument analysis*, CENGAGE Learning, Boston, U.S.A, 2016.

67 R. Bone, P. Cullis and R. Wolfenden, Solvent Effects on Equilibria of Addition of Nucleophiles to Acetaldehyde and the Hydrophilic Character of Diols, *J. Am. Chem. Soc.*, 1983, **105**, 1339–1343.

68 S. H. Hilal, S. N. Ayyampalayam and L. A. Carreira, Air - liquid partition coefficient for a diverse set of organic compounds: Henry's law constant in water and hexadecane, *Environ. Sci. Technol.*, 2008, **42**, 9231–9236.

69 R. Sander, Compilation of Henry's law constants (version 4.0) for water as solvent, *Atmos. Chem. Phys.*, 2015, **15**, 4399–4981.

70 S. Cornell, K. Mace, S. Coeppicus, R. Duce, B. Huebert, T. Jickells and L. Zhuang, Organic nitrogen in Hawaiian rain and aerosol ON m which makes up roughly one third of the total nitrogen in aerosol N m-3). The inorganic nitrogen as nitrate) is predominantly found in coarse-mode rainwater rainwater References :, *Pumps*, 2001, **106**, 7973–7983.

71 M. C. Facchini, M. Rinaldi, C. Carbone, S. Fuzzi, F. Moretti, E. Tagliavini, D. Ceburnis and C. D. O. Dowd, Important Source of Marine Secondary Organic Aerosol from Biogenic Amines, 2008, **42**, 9116–9121.

72 S. W. Gibb, R. F. C. Mantoura and P. S. Liss, Ocean-atmosphere exchange and atmospheric speciation of ammonia and methylamines in the region of the NW Arabian Sea, *Global Biogeochem. Cycles*, 1999, **13**, 161–178.

73 C. Müller, Y. Iinuma, J. Karstensen, D. Van Pinxteren, S. Lehmann, T. Gnauk and H. Herrmann, Seasonal variation of aliphatic amines in marine sub-micrometer particles at the Cape Verde islands, *Atmos. Chem. Phys.*, 2009, **9**, 9587–9597.

74 R. A. Di Lorenzo, B. K. Place, T. C. VandenBoer and C. J. Young, Composition of Size-Resolved Aged Boreal Fire Aerosols: Brown Carbon, Biomass Burning Tracers, and Reduced Nitrogen, *ACS Earth Sp. Chem.*, 2018, **2**, 278–285.

75 M. Rinaldi, S. Decesari, E. Finessi, L. Giulianelli, C. Carbone, S. Fuzzi, C. D. O'Dowd, D. Ceburnis and M. C. Facchini, Primary and Secondary Organic Marine Aerosol and Oceanic Biological Activity: Recent Results and New Perspectives for Future Studies, *Adv. Meteorol.*, 2010, **2010**, 1–10.

76 X. Lian, G. Zhang, Y. Yang, Q. Lin, Y. Fu, F. Jiang, L. Peng, X. Hu, D. Chen, X. Wang, P. Peng, G. Sheng and X. Bi, Evidence for the Formation of Imidazole from Carbonyls and Reduced Nitrogen Species at the Individual Particle Level in the Ambient Atmosphere, *Environ. Sci. Technol. Lett.*, 2021, **8**, 9–15.

77 C. E. Lawrence, P. Casson, R. Brandt, J. J. Schwab, J. E. Dukett, P. Snyder, E. Yerger, D. Kelting, T. C. Vandenboer and S. Lance, ACPD - Long-Term Monitoring of Cloud Water Chemistry at Whiteface Mountain: The Emergence of a New Chemical Regime, 2022, 1–31.

78 M. C. Facchini, S. Decesari, M. Rinaldi, C. Carbone, E. Finessi, M. Mircea, S. Fuzzi, F. Moretti, E. Tagliavini, D. Ceburnis and C. D. O'Dowd, Important source of marine secondary organic aerosol from biogenic amines, *Environ. Sci. Technol.*, 2008, **42**, 9116–9121.

79 S. W. Gibb and A. D. Hatton, The occurrence and distribution of trimethylamine-N-oxide in Antarctic coastal waters, *Mar. Chem.*, 2004, **91**, 65–75.

80 G. M. King, Methanogenesis from Methylated Amines in a Hypersaline Algal Mat, *Appl.*

Environ. Microbiol., 1988, **54**, 130–136.

81 B. P. Leaderer, L. Naeher, T. Jankun, K. Balenger, T. R. Holford, C. Toth, J. M. Wolfson and P. Koutrakis, Indoor, Outdoor, and Regional Summer and Winter Concentrations of PMJ F out Kerosene Space Heaters PM2.5', S 42-, H+, NH4+, NO3-, NH3, and Nitrous Acid in Homes with and without Kerosene Space Heaters, 1999, **107**, 223–231.

82 J. D. Spengler, P. Koutrakis, D. W. Dockery, M. Raizenne and F. E. Speizer, Health effects of acid aerosols on North American children: Air pollution exposures, *Environ. Health Perspect.*, 1996, **104**, 492–499.

83 M. Brauer, P. Koutrakis, G. J. Keeler and J. D. Spengler, Indoor and outdoor concentrations of inorganic acidic aerosols and gases, *J. Air Waste Manag. Assoc.*, 1991, **41**, 171–181.

84 Y. Li and R. M. Harrison, Comparison of indoor and outdoor concentrations of acid gases, ammonia and their associated salts, *Environ. Technol. (United Kingdom)*, 1990, **11**, 315–326.

85 F. Luceri, G. Pieraccini, G. Moneti and P. Dolara, Primary Aromatic Amines from Side-Stream Cigarette Smoke are Common Contaminants of Indoor Air, *Toxicol. Ind. Health*, 1993, **9**, 405–413.

86 G. Palmiotto, G. Pieraccini, G. Moneti and P. Dolara, Determination of the levels of aromatic amines in indoor and outdoor air in Italy, *Chemosphere*, 2001, **43**, 355–361.

87 J. Zhu and B. Aikawa, Determination of aniline and related mono-aromatic amines in indoor air in selected Canadian residences by a modified thermal desorption GC/MS method, *Environ. Int.*, 2004, **30**, 135–143.

88 M. Akyüz, Simultaneous determination of aliphatic and aromatic amines in indoor and outdoor air samples by gas chromatography-mass spectrometry, *Talanta*, 2007, **71**, 486–492.

89 R. E. O'Brien, Y. Li, K. J. Kiland, E. F. Katz, V. W. Or, E. Legaard, E. Q. Walhout, C. Thrasher, V. H. Grassian, P. F. Decarlo, A. K. Bertram and M. Shiraiwa, Emerging investigator series: Chemical and physical properties of organic mixtures on indoor surfaces during HOMEChem, *Environ. Sci. Process. Impacts*, 2021, **23**, 559–568.

90 W. W. Nazaroff and C. J. Weschler, Indoor acids and bases, *Indoor Air*, 2020, **30**, 559–644.